The Effect of Particle Shape and Size on the Stability of Pickering Emulsions

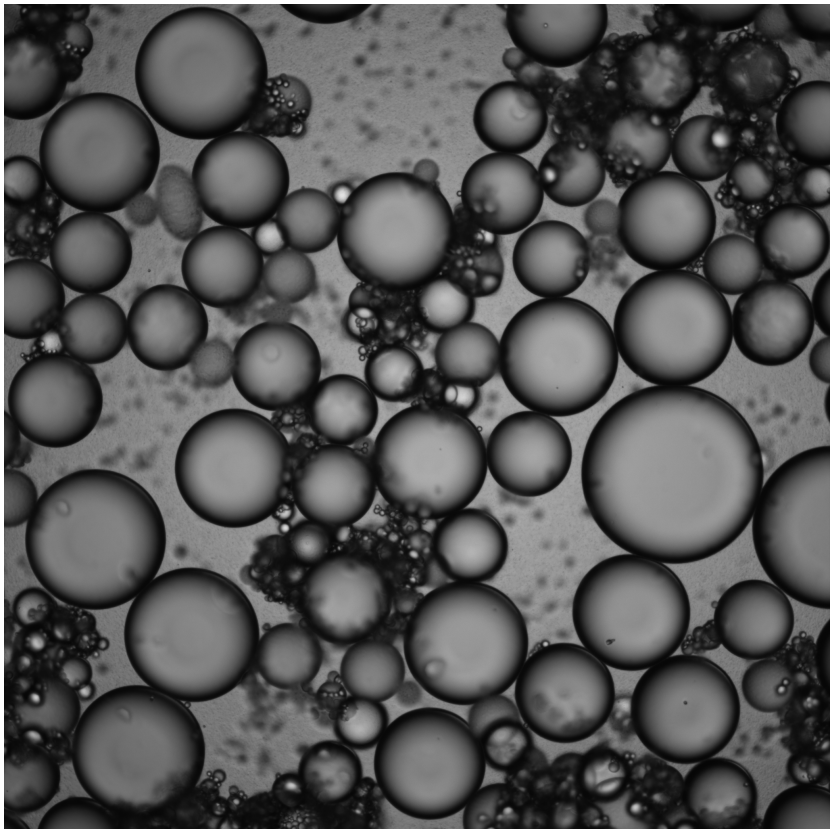

Hedera Dehlia Elisabeth Menger B. Sc.

04-11-2019

The Effect of Particle Shape and Size on the Stability of Pickering Emulsions

Hedera Dehlia Elisabeth Menger B. Sc.

Utrecht University

A thesis presented for the degree of
Master of Science

Student number: 6034896
E-mail address: h.d.e.menger@students.uu.nl

Van 't Hoff Laboratory for Physical and Colloid Chemistry
Debye Institute for Nanomaterials Science
University Utrecht

Under the supervision of
Riande I. Dekker M.Sc. & Prof. dr. W. K. Kegel
04-11-2019

NWO | Netherlands Organisation for Scientific Research

ISPT

Abstract

Emulsions are used in a wide variety of applications in the oil, food and cosmetic industry. They consist of two immiscible liquids where one liquid is dispersed in the other liquid. Pickering emulsions are emulsions where particles are adsorbed at the oil-water interface with a high stabilization energy and are believed to form a continuous layer around the dispersed drops impeding coalescence and hence stabilizing the emulsion. Extensive research has been performed in varying the composition, shape and size of the colloidal particles. In this research, we focus on cubic shaped particles to stabilize oil-in-water emulsions. Using optical and laser scanning confocal microscopy the adsorption and orientation of the cubic particles at the oil-water interface was studied. Whereas the hematite cubes with side lengths of around one micrometer stabilize emulsions with oil droplets of several millimeters, in this study oil droplets of micrometer sizes were observe when using copper oxide cubes of around 60 nm. Both types of cubes can serve as a template for the synthesis as hollow silica cubes, which were used to study the effect of particle size on the stability of oil-in-water emulsions.

Acknowledgement

Since the beginning of my master at the Debye Institute of Nanomaterials Science, I am fascinated by the research and development of sustainable cosmetics. My goal during this master was to develop enough chemical knowledge, especially about physical chemistry, and combine this with cosmetic experiences. Therefore, I was looking for a master thesis project that suits with this idea. Doing my master thesis at the Van 't Hoff laboratory for Physical & Colloid Chemistry (PCC) is a valuable opportunity. First and foremost, I would like to to thank Riande Dekker for giving me the opportunity to work on this fundamental project which can also be applicable in the field of cosmetics. Furthermore, I would like to thank prof. dr. W. K. Kegel for being my professor supervisor during my master thesis, providing valuable new insights and for hosting the Friday Brainstorm sessions. New results were presented and discussed with the whole brainstorm group, thank you all for the discussions about my thesis subject. I thank dr. Ben H. Erne for being my second supervisor. Furthermore, I would like to thank Frans Dekker and Daniel ten Napel from assisting me with the synthesis of respectively copper oxide and the hematite cubic particles. All the laboratory and writing work and the organisation at PCC could not have been possible without the help of Dominique, Kanvaly, Bonny and Marina. Special thanks to Sandrine and Nathalie who were sitting next to me in the master student room, for their motivation and support during lab time and after lab time and answering all my LaTeX questions. Next, I would like to thank all the other PhD'ers and students in the laboratory. Last, I would like to express my gratitude towards my family and friends; my mum and dad for their interest, good advice and support. My sister Iris, with whom I am doing a master at the same time and helping each other with provide a fresh look on things from a differne tperspective and my little brother, Rutger and sister, Dehlia who are doing their bachelor in Science. Finally, i would like to thank my friends for the collaboration during my master, their friendship and the hours writing in the laboratory and in the library.

Contents

Abbreviations

PE Pickering emulsions

o/w oil-in-water

w/o water-in-oil

TEM transmission electron microscopy

SDS sodium dodecyl sulfate

GTT gel trapping technique

SEM scanning electron microscopy

PDMS polydimethylsiloxane

Cu(acac)$_2$ copper(II)acetylacetonate

PVP polyvinylpyrrolidone

ETPTA ethoxylated trimethylolporpane triacrylate

1 Introduction

Emulsions are widely used in the industry or in the field of food, cosmetics, agricultural and the drug sector for applications such as coating, drug delivery systems, technological areas, health care products and petroleum production.[1,2,3,4,5] The nature of emulsion components (such as oil, water, emulsifiers, stabilisers) play a dominant role in the interaction between droplets and environmental changes, e.g., pH, ionic strength, and temperature.[2,5,6,7,8,9] They can cause significant changes in the force balance, thereby influencing emulsion stability.[7] Convention emulsions are the most commonly known emulsions stabilised by emulsifiers or surfactants.[5,7,10] These emulsions have difficulties in stability because they easily overcome the energy barrier after which the emulsion becomes unstable. This result in a two liquid phase system which is a thermodynamically stable state.[5,10,11]

Pickering emulsions were studied by Ramsden in 1903 and by Pickering in 1907, who published about the enhanced stability of these emulsions relative to convention emulsions.[12,13] The stability of the generally used emulsions can be improved by using structural emulsions which have the most similarities to these conventional emulsions.[12,13] Pickering emulsions are stabilised by solid particles adsorbed at the oil-water of water/oil interface instead of surfactants.[2,3,5,14] The application of Pickering emulsions has risen strongly over the last two decades which can be seen in figure 1.1.[1] The number of publications within the field of Pickering emulsions has strongly increased since 1907, which is not surprising due to the relative high kinetic stability.[1,10,15,16] This stability is reached by reducing the interfacial area between oil and water by covering the interface with adsorbed particles.[14]

Different types of spherical solid particles are generally stabilising Pickering emulsions.[5,7,10,11,17] The interfacial packing and the orientation of the solid particles play a role during the adsorption when a Pickering emulsion is formed, according Folter (2013).[14] In his study, solid spheres and cubes were used during the stabilisation of Pickering emulsions to investigate the effect of the particle shape.[14,18,19] With respect to spheres, cubic particles tend to have a dense interfacial packing and less free interfacial (oil-water) area.[7,14] Solid cubic particles increase the stability of Pickering emulsions due to the anisotropy of particles either terms of shape or surface chemistry.[20,21] Spherical particles have a changing contact angle and this can be explained as follow; when the height of a solid particle with respect to the fluid interface changes, the contact angle of a spherical colloid varies in every position. The study of the contact angle for cubic particles is done by calculating the cubical shape and determining the orientation of the particles during the adsorption.[5,14,22,23,24,25,26]

Particle anisotropy either in terms of shape or in terms of surface chemistry makes them a better candidate for Pickering emulsion stabilization, fabrication of photonic

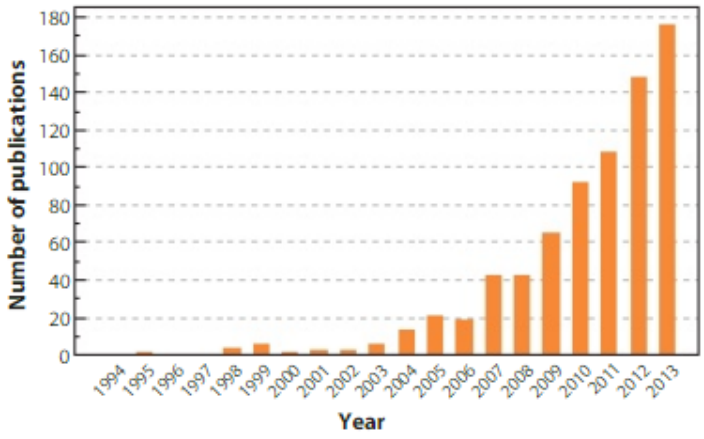

Figure 1.1: The increasing number of publications related to Pickering emulsions from 1994 till 2013.[1]

crystals, and in pharmaceutical applications.

Pickering emulsions are particle stabilised systems where colloids are adsorbed at the oil-water interface. As a consequence, they are ultra-stable since the particle-laden layer around the dispersed drops impede coalescence and hence stabilise the emulsions.[2,3,5,14,11] Extensive research has been carried out to study the impact of composition, shape and size of the colloidal particles on the stability of emulsions.[12,14] This study focuses on two types of colloidal cubes stabilisers, hematite cubes and copper oxide cubes, for oil-in-water emulsions with the goal of maximizing the packing/surface coverage and exploit capillary-driven interfacial rheology. Different types of microscopy are used to analyse the adsorption and orientation of the cubic particles at the oil-water interface.[14,22]

The aim of this study is to investigate the effect of the particle shape, size and composition on the stability of Pickering emulsions. Different colloidal particles are synthesized to study the mentioned effects, first hematite cubes and later copper oxide cubes. These cubes are coated in different ways to change the properties of the cubes. The particles are used to form Pickering emulsions after investigation by optical microscopy and transmission electron microscopy. In future work, emulsion stability will be investigated by rheology measurements and a new method, squeeze flow method, involving the confocal microscopy is presented where Pickering emulsions will be compared to surfactant-stabilised emulsions.[27]

2 Theoretical background

In this chapter, theoretical background information is provided which supports the purpose of this study.

2.1 Emulsions

Emulsion-based applications are studied in a wide range of disciplines, e.g. combining chemistry, biology, physics and engineering.[2,3,4,5] Many aspects from the field of science and technology are combined to study the fundamental principles of the behaviour of emulsions regarding polymer science, interfacial chemistry, colloid science and fluid mechanics.[4,8,9] Introducing the basics, emulsions are formed by the homogenisation of two immiscible liquid phases in which one of the liquid phases is dispersed into the other phase as small droplets. When an aqueous phase includes dispersed oil-droplets it is called an oil-in-water (o/w) emulsion and conversely, when the emulsion system is based on an oil phase with dispersed water droplets it is called a water-in-oil (w/o) emulsion. Homogenisation occurs when these two phases are completely mixed together which is achieved mostly by mechanically stirring in the industry. How emulsions are homogenised depends on the type of oil and water phase and on the type of surfactants or emulsifiers used for the formation of emulsions. After homogenising, the stability of the homogenised emulsion is time-related, it can be stable for a few seconds, minutes or even months. Conventional emulsions are stable if the energy barrier is higher than the thermodynamically unstable system can overcome and droplets are homogenised in the bulk phase. In a thermodynamically unstable system, the strong interfacial film between water and oil molecules and the driving force of the stabilisers (surfactants or emulsifiers) ensure that the droplets have no tendency to merge. These emulsions are kinetically stable because the droplets encounter strong Brownian motion which counteracts the phase separation of the oil and water phase.[5,10] By increasing the surface area, it affects the stability and therefore the emulsions becomes thermodynamically unstable. Thermodynamically unstable emulsions which have a higher state in free energy (ΔG_f), need to increase their free energy above ΔG^* to be a thermodynamically favoured system. In case ΔG^* becomes too large, it is impossible for the system to overcome the energy barrier used as a result of which the emulsion is kinetically stabilised in the thermodynamically unfavourable state.[5,10] When this thermodynamically unstable system overcomes the energy barrier, a thermodynamically stable system is formed which is no longer an emulsion (figure 2.1). During the first part of the phase separation process, the decreased free energy of the system is converted into interfacial free energy. The remaining available free energy is converted into kinetic energy of fluid motion to overcome the energy barrier. The formation of two liquid phases are driven

by the transferred energy of the reduction of surface area (interfacial area) into kinetic energy (via coalescence), which leads to a preferred thermodynamically stable state.[15] When an emulsion reaches the ΔG^* state it can change to a thermodynamic stable and kinetically unstable state. This last mentioned state is the lowest in energy and therefore the most favourable state.[5,10] Emulsion applied systems are rarely at thermodynamic equilibrium due to the structural organisation of surfactants or emulsifiers provide various kinetic energy barriers that prevent the system from reaching the lowest free energy.[15]

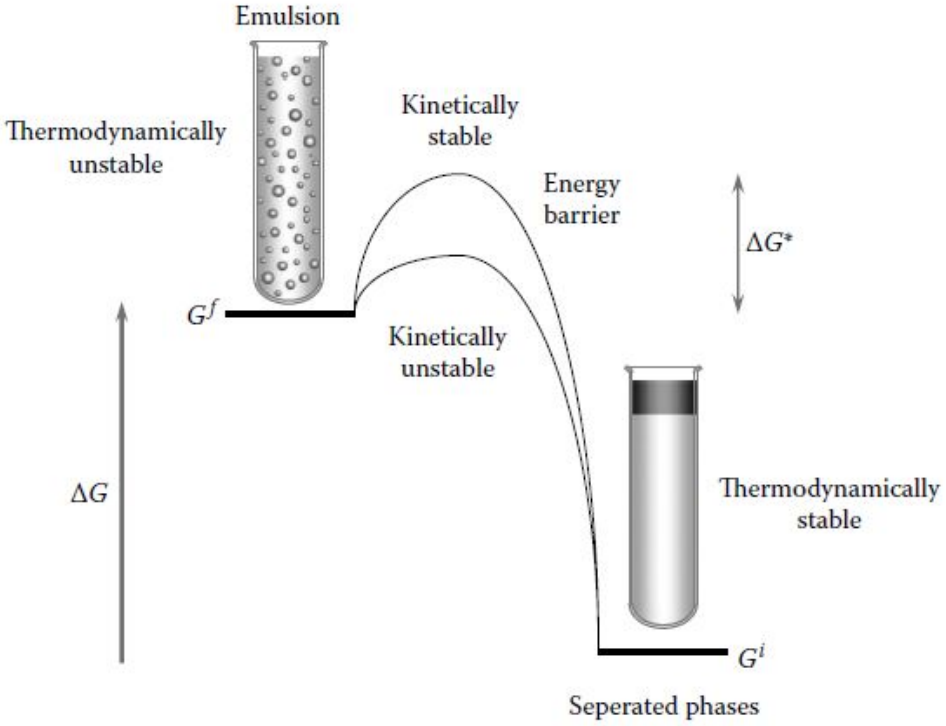

Figure 2.1: Energy barrier of the destabilisation of emulsions between thermodynamic and kinetic stability. The emulsions can stay in a thermodynamically unstable state if ΔG^*, the energy barrier, is high enough to avoid deformation to a thermodynamically stable emulsions.[5,10]

The difference between thermodynamic stability and kinetic stability in terms of free energy, ΔG is clarified by Eqn. 2.1. Emulsions that have the lowest free energy, ΔG_i, is the thermodynamically preferred state which is expressed as ΔG_i in figure 2.1.

$$\frac{n_f}{n_i} = \exp\left(-\frac{(G_f - G_i)}{kT}\right) \tag{2.1}$$

The thermodynamic stability of emulsions is time-related and depends on the reaction rate but it does not say anything about the rate of the changing properties of emulsions, the type of instability, or the physical mechanisms.[5,10,16] This increases the importance of the kinetic stability with respect to the thermodynamic stability. Despite the fact that emulsions are thermodynamically unstable, emulsions have an increasing kinetic stability when they consist of small droplets with a life extension instead of bigger droplets.[5,10] Smaller droplets have a larger overall surface area relative to bigger droplets or the overall surface area reduced due to coalescence by merging of the

droplets after which surface energy is released and converted to kinetic energy. Smaller droplets that coalesce overcome the energy barrier more easily than bigger droplets due to their higher energy release.[16]

2.1.1 Emulsion stability and possible destabilisation mechanisms

The most commonly used emulsions are surfactant-stabilised emulsions. Destabilisation of an emulsion occurs when emulsions are modified to a thermodynamically stable state. This destabilisation process, schematically illustrated in figure 2.2, can be influenced by various factors namely creaming, sedimentation, flocculation, phase inversion, coalescence or Ostwald ripening.[5,10]

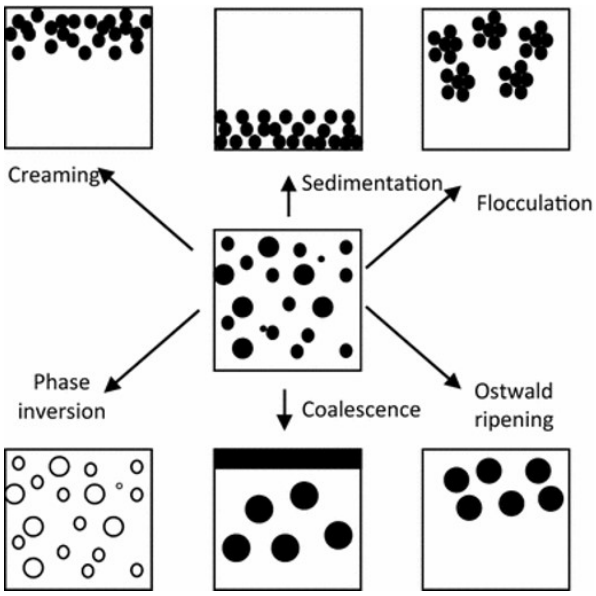

Figure 2.2: Types of different physical instabilities that can occur in emulsion systems.[5,7,10]

Emulsions that are separated into two phases is mainly caused by a coherence of physical instabilities.[5] Creaming of an emulsion is often emerged from severe coalescence, where coalescence is caused by the tearing of the interfacial films of emulsions. A separate layer arises apart from the bulk phase which is made due to the bigger droplets that move faster upwards than smaller droplets. During coalescence, bigger droplets are formed by merging two of more smaller droplets into one droplet where they lose their interfacial film. Not only coalescence generates creaming, but also polydispersed droplets and density differences between the oil and water phase. The reversal of creaming is sedimentation, dependent on the density of the dispersed phase with respect to the continuous phase. However flocculation has a different destabilisation mechanism, it ultimately results in the formation of bigger droplets and creaming. The only difference is that the droplets do not lose their interfacial film and merge together in one droplet. Flocculation is the effect of a strong van der Waals attraction which further increases by limiting the distance between the droplets.[5,10]
In o/w emulsions including polydispersed droplets, the small droplets diffuse towards the bigger droplets in the bulk. The phenomenon where oil droplets increase at the

expense of the smaller droplets which eventually leads to phase separation is called Ostwald ripening.[5,7] The larger particles are thermodynamically and spontaneously formed since the smaller particles in the emulsion were not energetically stable and eventually, small droplets disappear and big droplets grow. Phase separation and sedimentation take place when gravitational forces overcome Brownian motion. Furthermore, the differences in density between the oil and water phase is an important reason for phase separation. Changing the emulsion from oil-in-water to water-in oil or the other way around, is characterised as phase inversion.[10] This can appear in case of modification or variation of the emulsifier or surfactant. For example, some emulsifiers can change from hydrophilic to more hydrophobic by changing the temperature.[5,7,10]

Ways to increase the stability of emulsions are to strengthen the mechanical properties of the interfacial films by increasing the polymer adsorption at the interface, by increasing the electrostatic or by hindrance repulsion between droplets to decrease the result of flocculation. The difference in density resulting in creaming or sedimentation could be remedied by using weighting agents in the oil phase to even the density of the water phase. Moreover, the addition of thickening agents and increasing the mechanical forces can respectively increase the viscosity and decrease the droplet size which at the end reduce the phase separation. The viscosity depend on the droplets size; large droplets lead to an increasing emulsion viscosity and induce creaming.[5,6]

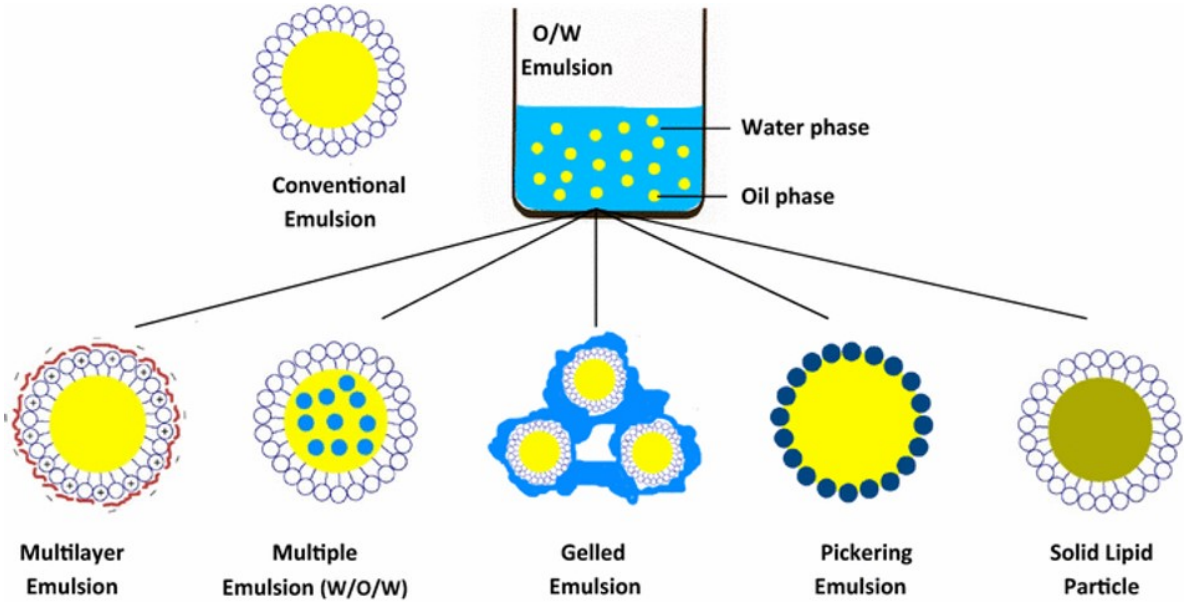

Figure 2.3: Schematic presentation of ways to improve the stability of conventional emulsions by making use of structured emulsions. The most common alternative emulsions are multilayer emulsions, multiple emulsions, gelled emulsions, Pickering emulsions and solid lipid particle emulsions.[7]

The conventional emulsions are prone to several types of instabilities, coalescence, creaming, flocculation, Ostwald ripening, phase inversion and sedimentation, as described before.[7] These instabilities can easily cause destabilisation over time, therefore structured emulsions are developed to improve the stability of conventional emulsions. Limiting the causes of the instability is realized by using one of the following types of emulsions, multilayer emulsions, multiple emulsions, gelled emulsions, Pickering emulsions or solid lipid particle emulsions shown in figure 2.3.[5,7] The advantage of a multi-

layer emulsion is a better conservation against among others, heating, change in pH or high ionic strength. This can be explained by using a multilayered interface around the oil droplets in the emulsion which has the advantage of a low polydispersity and a less oil leakage from the droplets.[28] Multiple emulsions are described as double emulsions which can occur as water-in-oil-in-water (w/o/w) emulsions or as oil-in-water-in-oil (o/w/o) emulsions.[7] These emulsions have two contrasting interfacial films, one at the oil-water interface and the water-oil interface. Although, the double emulsions are in a thermodynamically unstable system, multiple emulsions give even more stability due to the better encapsulation efficacy and the limiting of the leakage of oil or water.[29] In gelled emulsions the oil droplets are captured by the gel phase to slower down the transfer and the diffusion. For the formation of gelled emulsions is a conventional emulsion synthesised whereafter for example a polymer can be added.[6] Solid lipid particle emulsions have similar characteristics to the traditional emulsions with liquid oil particles. Again, this type of emulsion is formed as a conventional emulsion and later cooled down to stimulate the lipid crystallisation. In comparison with gelled emulsions, the crystalline oil phase does not contain solid lipid particles because the particles are dispersed in the water phase and yet, solid lipid particle emulsions do have similar physical barriers. The last type of structured emulsions are Pickering emulsions. In this type of emulsions instead of a surfactant, it uses solid particles to stabilise the oil-in-water (o/w) of water-in-oil (w/o) emulsions. The Pickering emulsions have the most affinity with traditional emulsions because the attachment of solid particles on the oil-water interface is similar to the surfactant behaviour.[11] The partial wetting functionality of the solid particle ensures that the interface between water and oil is mechanically stronger. Besides this, Pickering emulsions are spontaneously formed if the preferable particle size is smaller than the emulsion droplet size. The advantage of the solid particles is the fast decreasing interfacial area between oil and water during the homogenisation of the emulsion which highly increase the stability so it can be stored for longer time.[30]

2.1.2 Pickering emulsions vs. surfactant stabilised emulsions

Pickering emulsions (PE) are more often used instead of the surfactant-stabilised emulsions and they are applied in many studies.[2,3,4,5,8,9] The advantage of using Pickering emulsions instead of conventional or surfactant-stabilised emulsions is that less harmful solid particles are required to reduce the amount of hazardous surfactants. In addition, the emulsifying agents could be either lowered in concentration or completely removed from the emulsions when using Pickering Emulsions.[17] Different studies on solid stabilised emulsions have published general regulations and are summarised as followed;[14,18,19,20,21]

The characteristic solid particle size has to be significantly smaller than the size of water or oil droplets of its emulsion. Then, the wettability of the particles must be partial in the oil and the water phase to form a stable and efficient emulsion. According to Finkle (1923),[31] the colloidal particles in emulsions are more wetted by one preferred phase and the phase with the least wettability is the dispersed phase. Furthermore, the type of emulsion, oil-in-water or water-in-oil, is induced by the added oil-water volume ration. When the volume fraction of the dispersed phase increases, it promotes phase inversion. For each emulsion, the inversion point is affected by changes in wettability, stability and particle size distribution. These variable are very important for the determination of the inversion point of the oil-water phase.[17,32] Moreover, emulsions with

small droplets are relatively stable because the droplets experience a balance between attractive and repulsive forces from their neighboring droplets. The commonly known attractive forces are hydrogen bonding and electrostatic interactions and the repulsive known forces are among others, hydrophobic attraction, steric hindrance, and electrostatic repulsion.[7]

The biggest difference and most important reason to use Pickering emulsions is that they are not stabilised in a physical way as described for stabilised emulsions.[10] The stability of Pickering emulsions is caused by partly wetting of solid colloidal particles between the oil and water phase. In this way PE are more stable and have an increasing interfacial thickness and surface load (mg/m^2) compared to the typically values of the surfactant-stabilised interfaces.[2,5] Surfactants-stabilised emulsions need to undergo high forces to homogenise the two phases. While this happens, surfactants assembled in the water or oil phase are adsorbed onto the surface of the droplets. Hereby, the interfacial tension of the created droplets decreases and at the same time stabilising interfacial films are formed, aggregation of newly formed droplets is prevented and the emulsion tends to be stable. This conventional emulsion is a stable emulsion, however, after a period of time the emulsion destabilises in two separate layers caused by various factor such as, concentration surfactant, temperature, pH, homogenisation parameters or ionic strength.[5,7] Pickering emulsions form spontaneously after manual shaking when the system conditions are as preferred. This is the result of the high stability against coalescence because the interfacial tension is constant for Pickering emulsions and the adsorbed solid particles provide a reduction in interfacial area.[22] By using nanometric or micron-sized solid particles the emulsion droplets can be smaller related to traditional emulsions which is the most advantageous difference.[23] Another similarity is the adsorption that takes place at the oil-water interface. In both conventional emulsions as Pickering emulsions is explained that respectively surfactants and solid colloidal particles are adsorbing at the oil-water interface. Both emulsions have a similar attachment behaviour on the oil-water interface.[23] However, the adsorption mechanism is different in both cases since the surfactant molecules have a amphiphilic character. The structure of surfactants, hydrocarbon chain with a polar head group, enables the adsorption at the interface between the nonpolar and polar liquids. Colloidal solid particles do not have to be amphiphilic because the interactions necessary for adsorption at the interface for solid particles are based on the properties of the particles' surface.[11,23]

2.1.3 Pickering emulsions and particle wettability

Different improvements are studied to enhance the stability of emulsions.[5,6,7,10,28,29,30] One is used for the focus of this research, namely Pickering emulsions. Pickering emulsions (PE) are emulsions with the same oil-water interfaces as described in section 2.1 but the crucial difference is that these emulsions are not highly stabilised by surfactants but by solid colloidal particles. In order to form a continuous layer around the dispersed drops to impede coalescence and hence stabilise the emulsion.[22]
This phenomenon where solid particles were adsorbed at the fluid interface was first documented by Ramsden in 1903.[12] After this study, the groundbreaking article from Pickering was published in 1907. This was decisive for naming the invented emulsions after Pickering instead of Ramsden.[13]

As described before, stable Pickering emulsions have adsorption of particles at the interface between oil and water. The behaviour of the particle adsorption at and desorption from at the fluid-fluid interface is dependent on the balance between the interfacial tensions of the oil-water, solid/oil and water/solid interfaces as respectively γ_{ow}, γ_{so} and γ_{ws}.[23] This equilibrium is using θ as contact angle in the Young's equation;[24]

$$\gamma_{ow} \cos\theta = \gamma_{so} - \gamma_{ws} \tag{2.2}$$

If particles have no preferred wettability the contact angle is 90°, which is the most stable situation for PE. Oil-in-water emulsions occur when $\theta < 90°$, having a solid/oil tension γ_{so} which is greater than the water/solid tension γ_{ws}, that indicates the adsorption of hydrophilic colloidal particles. For hydrophobic particles, $\gamma_{so} < \gamma_{ws}$ and $\theta > 90°$ lead to the formation of water-in-oil emulsions.[24]

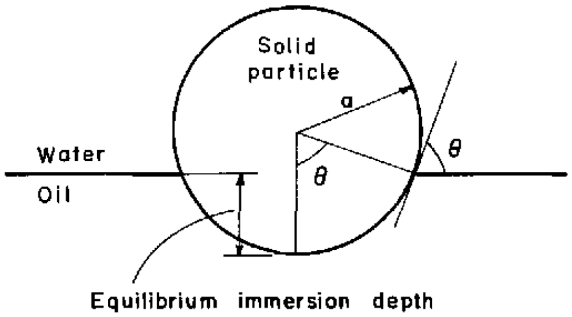

Figure 2.4: Schematic representation of a single solid particle adsorbed at a fluid-fluid interface and partially immersed in both phases. The radius is expressed as a (figure) and as r (text and equations).[24]

An oil-in-water emulsion is used as the basic where a spherical single particle with radius r adsorbed at the interface is an assumption in the equations (figure 2.4).[24] The height of a colloidal particle with respect to the interface can vary due to differences in wettability.[21,24] To reach the equilibrium immersion depth for a stable emulsion, a particle must partially be immersed in both the oil and water phase. This equilibrium immersion depth is equal to $(1 - cos\theta)$, for part one (solid/oil interfacial tension) and part two (water/solid interfacial tension) of equation 2.3. The third part of the equation, $\gamma_{ow} \sin^2\theta$, is the energy lost from the removed area, $\pi r^2 \sin^2\theta$, of the oil-water interface to adsorb the solid particle.[24] In the following situation, external forces (e.g. gravity) and rounded interfaces are neglected. When a particle is adsorbed at the interface it has generated a gain in energy, therefore the interfacial energy can be expressed as follows,[24]

$$\Delta G = \pi r^2 [2\gamma_{so}(1 - \cos\theta) + 2\gamma_{ws}(1 + \cos\theta) - \gamma_{ow} \sin^2\theta] \tag{2.3}$$

Filling in Young's law, equation 2.2, into equation 2.3 the interfacial energy becomes;

$$\Delta G = 4\pi r^2 \gamma_{ws} - \pi r^2 \gamma_{ow} (1 - \cos\theta)^2 \tag{2.4}$$

The first part of equation 2.4 is the interfacial energy of a spherical particle totally immersed in the water phase. The second term is the change in interfacial energy due to the movements of a particle from the bulk phase to the interface which can also

be appointed as the desorption energy. This is defined in the next relationship for a spherical particle at a planar interface.[25]

$$\Delta G = \pi r^2 \gamma_{ow} (1 \pm \cos\theta)^2 \tag{2.5}$$

This energy, the size of the displaced area, is based on the size and shape of the colloidal particles and contact angle with both fluids. A new oil-water interface must be created by removing an adsorbed particle which has a free energy cost. When $1 \pm \cos\theta$ has a positive sign in the equation which is in agreement with the removal into the oil phase and when $1 \pm \cos\theta$ has a negative sign it refers to the removal of the aqueous phase.[26]

2.1.4 Investigation of emulsion stability

Squeeze flow method

Dekker et al. (*in preparation*) studied emulsion stability by analysing when destabilisation of the emulsion occurs.[27] During the squeeze flow experiment, the sample thickness of the emulsion is slowly decreased to below the droplets diameter which is illustrated in figure 2.5. At some point, the sample thickness, e, between two glass plates, a thick glass plate of 1 mm and a thin microscope cover glass slide of 170 µm, is reduced by squeezing. In case of an o/w emulsion the water is mechanical squeezed out and the droplets of the emulsions deform and become unstable. This method gives an indication about the stability of the emulsion. The destabilisation of a sodium dodecyl sulfate (SDS)-stabilised emulsion is pictured in figure 2.5. Coalescence starts to occur between the confocal microscopy images C and D where the critical coalescence point is referred as e_c at a height distance between 11 µm and 12 µm.[27] A height-adjustable rheometer is used to control the position. It is observed that the emulsion droplets start to coalesce if $e > e_c$.[27] This squeeze flow experiment was originally used as a new technique to analyse the flow properties of non-Newtonian fluids.[33]

In this study, the squeeze flow technique can be a suitable method to investigate the stability of the Pickering emulsion droplets and compare the results of the Pickering emulsions with the results of the SDS-stabilised emulsions.

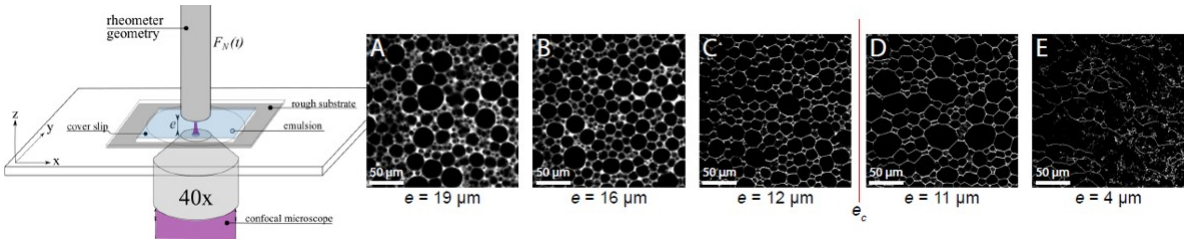

Figure 2.5: Schematic setup and pictures of a SDS-stabilised emulsion analysed by confocal microscopy during a squeeze flow experiment. The emulsion in images A to E is used to study the stability of the emulsion droplets by their coalescence under pressure. This pressure is created by lowering the sample thickness or height (e) between the rheometer and the lower glass plate. Eventually, the critical sample thickness, e_c is reached after which the emulsion destabilise.[27]

2.2 Colloidal cubes

All theory so far is defined and explained with the assumption that hard spherical colloids are used for Pickering emulsions. This study is focussing on Pickering emulsions stabilised by cubical solid particles adsorbed at the liquid-liquid interface. The cubes form a higher densely packed particles-laden interface in the emulsions relative to spherical solid particles. Different types of cubical colloids, hematite cubes, copper oxide cubes and hollow cubic silica particles are used to study the effect of the particle's shape, size and chemical composition on the stability of the formed Pickering emulsions.[14,34]

2.2.1 m-values

Since the particles are not perfectly cubic, the particle shape parameter m is used to determine the cubicity of the colloids.[19] This parameter is part of the superball equation which is represented as

$$|\frac{x}{r}|^m + |\frac{y}{r}|^m + |\frac{z}{r}|^m = 1, \tag{2.6}$$

Where r is defined as the radius of the superball particle. The m-value of the rounded cubes can be calculated from the aspect ratio (AR), which is the ratio between the diagonal b and the edge-length a, with the following equation;

$$AR = \frac{b}{a} = \sqrt{2}(\frac{1}{2})^{\frac{1}{m}} \tag{2.7}$$

The equations can be calculated for the deformation of a sphere into a cubic particle.[19] The cubicity of a colloidal particle can be rewritten to get the m-value as function of AR.

$$m = \frac{-\log 2}{\log AR - \log \sqrt{2}} \tag{2.8}$$

The deformation with different m-values are shown in the schematic illustrations of figure 2.6.[19] This parameter is 2 for a spherical particle because the spherical radius equals to the particle radius. When m approaches infinity the particle radius becomes half of the edge-length and the superball is forming a perfectly cubic particle, d=2r.[19,35,36]

2.2.2 Contact angle

As described so far, the wettability of the solid particles adsorbed at the oil-water interface is an important parameter quantified by the contact angle θ. For spherical particles, the contact angles change with every small deviation in the position of the particle at the interface. It becomes increasingly interesting when particles are used with a cubical shape because their straight side length provide a constant contact angle, only around the corner the contact angle change. Therefore, the contact angle only changes if the wettability of one of the two liquid phases is strongly dominated and the contact angle is determined by the rounded corners of the cubical particles. This is shown in figure 2.7a and 2.7b, where the contact angle is modified in figure 2.7a and remains unchanged in figure 2.7b.[22,14]

There are three possible conditions for the contact angle as mentioned in paragraph 2.1.3. Colloidal particles adsorbed at the interface from an o/w emulsions have a contact

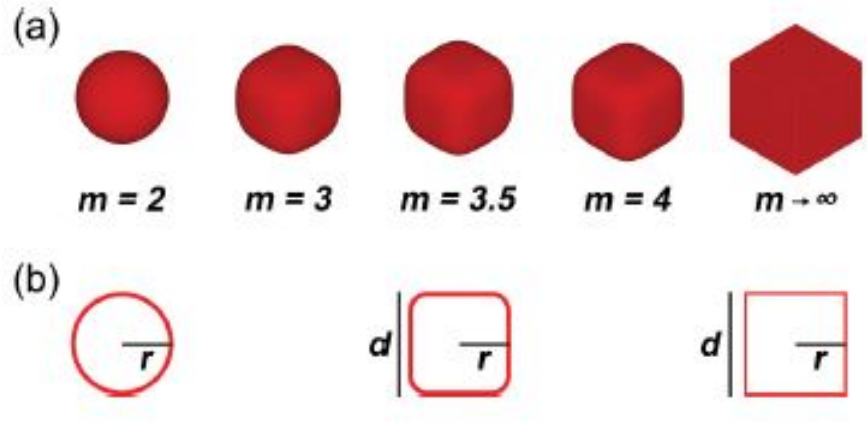

Figure 2.6: Schematic representation of the calculated m-values and the value on the shape of a colloidal superball by expressing the deformation parameter m. (a) a spherical particle starts with $m = 2$ and changes to a perfect cubes with $m \to \infty$. (b) the 2D-illustration of the particles with d as diameter and r as radius of the (rounded) cube.[19,35,36]

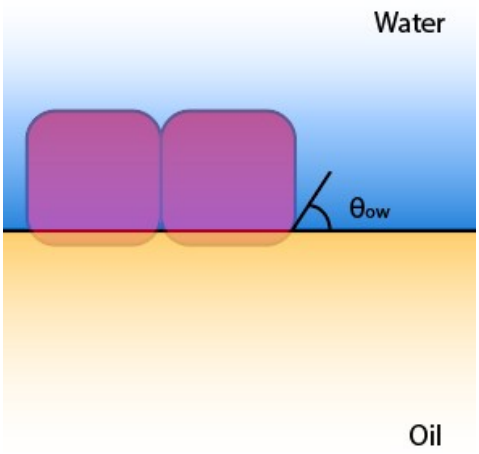

(a) Changed contact angle by the roundness of the corners of the cubes.

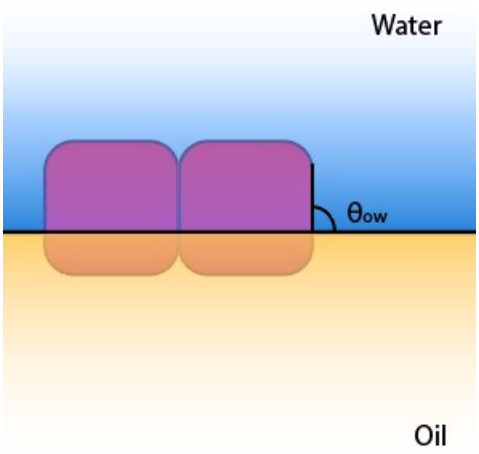

(b) Cubic particles with a solid contact angle of 90°at the side length of the cubes.

Figure 2.7: Schematic images show change in the contact angle when a Pickering emulsion is stabilised by colloidal cubes which have a [100] particle orientation with respect to the oil-water interface. In situation (a) the contact angle change if there is a variation is height with respect to the interface and in situation (b) the contact angle is stable when the cubic particle has a small variation is the height with respect to the interface.

angle θ slightly lower than 90°. The particles preferentially wetted by the water phase are hydrophilic particles. At last, if the particles provide a w/o emulsion than θ is slightly bigger than 90°and the solid stabilisers are hydrophobic. As previously stated, the hydrophobicity or hydrophilicity determines the contact angle (θ) of solid particles and ensures that particles remain at the interface. Particles dispersed in the aqueous phase become more hydrophilic and particles dispersed into the oil phase become more hydrophobic. Another condition, if particles do not have a preference for a liquid phase,

no dominance, the cubic particles have a contact angle of 90°. These conditions provide that the assumption can be made that the cubic shape of the adsorbed particles have a big influence on the packing behaviour.[14,32]

2.2.3 Reaction mechanism of hematite cubes

One of the solid colloidal cubes used during this study are the red hematite cubes. The synthesis of hematite cubes is carried out in an aqueous environment where $FeCl_3 \cdot 6\,H_2O$ in H_2O is mixed with a dissolved aqueous NaOH solution.[19,35,36] The formation of the precipitate, $Fe(OH)_3$ is expressed in reaction equation 2.9 and 2.10. It reacts into hematite needles, akaganeite ($\beta-FeO(OH)$), see process 2.11. Eventually, the formation of akaganeite into cubic hematite colloids, $\alpha-Fe_2O_3$, occurs which is shown in reaction equation 2.12.[37]

$$FeCl_3 \cdot 6\,H_2O + 3\,NaOH \longrightarrow {Fe^{3+}}_{(aq)} + 3\,{Cl^-}_{(aq)} + 3\,{Na^+}_{(aq)} + 3\,{OH^-}_{(aq)} + 6\,{H_2O}_{(l)} \quad (2.9)$$

$${Fe^{3+}}_{(aq)} + 3\,{OH^-}_{(aq)} \longrightarrow {Fe(OH)_3}_{(s)} \quad (2.10)$$

$${Fe(OH)_3}_{(s)} \longrightarrow \beta-{FeO(OH)}_{(s)} + {H_2O}_{(l)} \quad (2.11)$$

$$2\,\beta-{FeO(OH)}_{(s)} \longrightarrow \alpha-{Fe_2O_3}_{(s)} + {H_2O}_{(l)} \quad (2.12)$$

Hexaaquairon(III) ion is formed during side reactions and acts like an aqua acid (figure 2.8). The molecule has a Brønsted acid behaviour where an acid proton of the water molecule interacts with the central Fe-ion. Thereby, the $[Fe(H_2O)_6]^{3+}$ complex has achieved the maximum oxidation state of nonorganometallic complexes of the d-metals and rearranges until the favourable oxidation state of 3 ($Fe(OH)_3$) is reached.[37]

$${[Fe(H_2O)_6]^{3+}}_{(aq)} + {H_2O}_{(l)} \rightleftharpoons {[Fe(H_2O)_5OH]^{2+}}_{(aq)} + {H_3O^+}_{(aq)} \quad (2.13)$$

Reaction 2.13 can be explained by representing the metal cation as a sphere with radius r containing positive charges. The hexaaquairon(III) ion complex is a strong aqua acid that weakens by reducing the positive charge of the central metal ion and increasing ionic radius into a Fe^{2+} complex. The induced effect of the Fe-core positively influences the removal of the protons from the vicinity of the highly charged Fe-ion with a small radius. This process, mechanism 2.8c, continues until the $Fe(OH)_3$-complex is formed which is represented in figure 2.8.[37] The proton donation from the iron complex to the water phase during the synthesis as shown in figure 2.8.c.[37] This negatively affects the pH of the colloidal hematite suspension and the aqueous solution becomes acidic.[36,38,37] Eventually, the relatively low pH inhibits the formation of Pickering emulsions. Therefore, increasing the pH of the suspension between 4 and 7 by washing is necessary after the formation of hematite cubes.

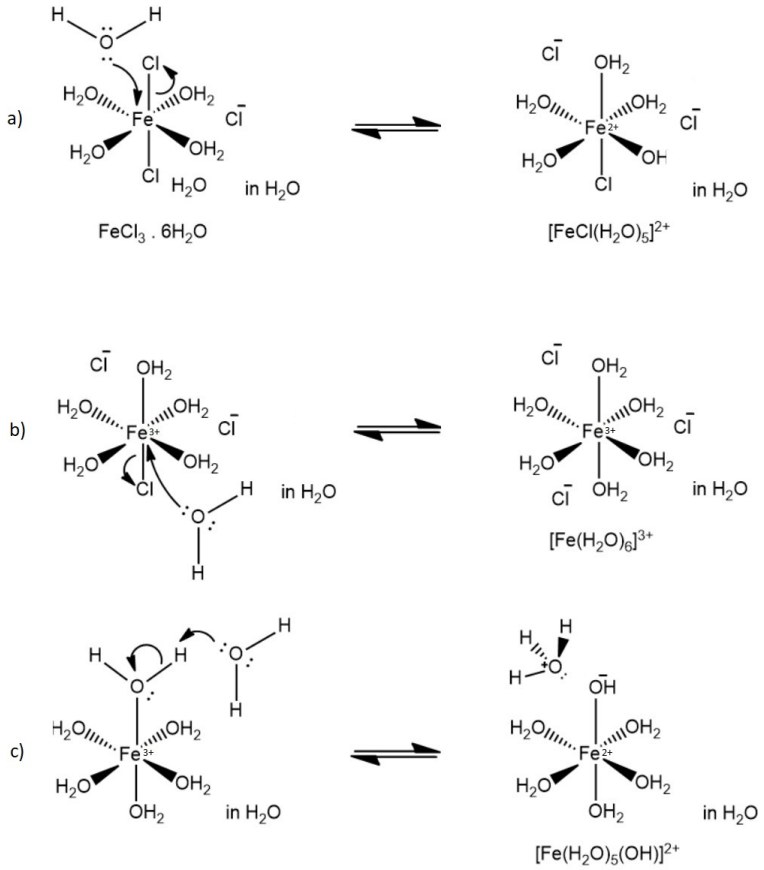

Figure 2.8: Reaction mechanism of a part of the hematite synthesis with (a) and (b) the formation of the hexaaquairon(III) ion complex and (c) the mechanisms of the transformations from $[Fe(H_2O)_6]^{2+}$ to $[Fe(OH)_3]$.[37]

2.2.4 Reaction mechanism of copper oxide cubes

The other solid colloidal cubes used during this study are orange/yellow copper oxide cubes. Many methods are used in the past to synthesis Cu_2O particles in various shapes.[39,40,41] In 2003, uniform cubic nano-particles with a size of 200 - 450 nm were produced according a wet synthesis, the first reported by Gou and Murphy.[42] During this synthesis they reduced Cu(II) salts in H_2O using $C_6H_7NaO_6$, sodium ascorbate, to form cuprous oxide nanocubes between 0.5 and 5 µm. In 2015, a substituted method for metal oxide particles with various shapes is discovered by Dong, Chen and Fledmann. This method, the "polyol method" is reducing the metal salts with a di-alcohol under high temperature conditions.[43] The adapted polyol method by Park et al. (2009) is employed to synthesis cubic copper oxide particles within a size range of 50 and 100 nm.[44] A detailed mechanism seems to be unknown for the synthesis of copper oxide cubes adding 1,5-pentanediol to copper(II)acetylacetonoate in the presence of polyvinylpyrrolidone. Only two steps are repeatedly mentioned during the reduction of the polyol method; the first step in the formation of an aldehyde from the polyol during dehydration and subsequently reduced forming a diketone.[45,46] The proposed reaction equation from $Cu(acac)_2$ yielding into Cu_2 by the polyol reduction (2.14 and 2.15).[35]

$$OH{-}C_4H_8{-}CH_2OH \xrightarrow{\Delta} C_4H_9{-}CHO + H_2O \tag{2.14}$$

$$4\,Cu^{2+} + 6OH^- + 2C_4H_9{-}CHO \longrightarrow 2\,Cu_2O + C_4H_9{-}CO{-}CO{-}C_4H_9 + 4\,H_2O \tag{2.15}$$

2.2.5 Reaction mechanism of silica coated particles

Silica coatings on nanoparticles have been applied for a long period of time to enhance the colloidal particle stability and chemical resilience.[47] The silica coated synthesis for nanoparticles was original reported by Stöber et al. (1968).[48] Stöbers experiments were produced by chemical reactions of tertaesters of silic acid which was based on previous work with tetraethyl silicate. The precursor used for Stöber silica synthes in this study is tetraethyl orthosilicate (TEOS). The reaction equations 2.16 and 2.17 required for the formation of silica coated particles showed the hydrolysis of TEOS and a condensation reaction.[48,35]

$$Si(OEt)_4 + H_2O \longrightarrow HO{-}Si(OEt)_3 + EtOH \tag{2.16}$$

$$(EtO)_3Si{-}OH + HO{-}Si(OEt)_3 \longrightarrow (EtO)_3Si{-}O{-}Si(OEt)_3 + H_2O \tag{2.17}$$

2.3 Characterisation of the colloidal cubes

In this section, the theoretical background of the analysis methods used for the study of the synthesised cubic particles and the formed Pickering emulsions is described.

2.3.1 Optical and fluorescence microscopy

Optical microscopy is mostly known as light microscopy and it is used in this study for making enlarged images of solid particles and oil and water droplets of Pickering emulsions. A relative low sample concentration is used to visualise and characterise individual particles. For fluorescence microscopy, two extra filters, where the light can pass though, are needed while combining it with optical microscopy. Cubical colloids that are labeled with a fluorescent dye to visualise the silica coating for analysing the shape and size and to study the orientation on the oil-water interface of a emulsion droplet. The light beam with a particular excitation wavelength illuminates the sample. The dyed object is imaged when the emitted fluorescence is detected.[49,50] Hematite cubic particles with edges around 1 µm can be analysed by optical microscopy, which is in contrast to copper oxide cubes with a size range variable between 40 nm and 120 nm.[35]

2.3.2 Laser scanning confocal microscopy

Optical microscopy is only imaging the outer surface of the oil and water droplets and the particles. This technique makes it hard to study the cubes' adsorption at the interface in detail. Thereby, the particles and emulsion droplets are further visualised by laser scanning confocal microscopy (LSCM) for a determination of the particles orientation with respect to the oil-water interface. While using LSCM, a laser beam provides a small point of high intensity light is scanning the sample by using a specialised type of fluorescence microscope. It is only possible to focus the beam at one point at a specific depth of the sample and the detector only allows emission from the same focused point to create a fluorescent dyed image. This gives the image a better resolution because confocal microscopy avoids stray light.[49,50]

2.3.3 Transmission electron microscopy

In principle, transmission electron microscopy (TEM) is similar to optical microscopy except for two required parts. The beam of light is replaced by a beam of electrons which is produced by a cathode and secondly, the TEM uses magnetic coils to focus the beam instead of the lenses of glass. A ultra thin sample or a low concentrated suspension on a grid, is placed in vacuum where the beam is transmitted through the sample. The electrons are adsorbed and/or scattered from the beam as it passed through the sample to make high resolution images with a good contract. Electron microscopes have a larger image resolution and can image relative smaller particles with respect to optical microscopy. This technique can image small particles up to a minimum diameter of 2 nm.[49,50]

2.3.4 Gel trapping technique

Several methods for characterizing the contact angle exist and are used nowadays but the results of these techniques are hard to analyse and to translate into the contact angle.[51,52,53] According to Cayre and Paunov (2004), there is an easier, quicker and more applicable way to measure the contact angle of the colloidal particles at the oil-water interface. This method is called the gel trapping technique (GTT) which is schematic represented in figure 2.9.[54]

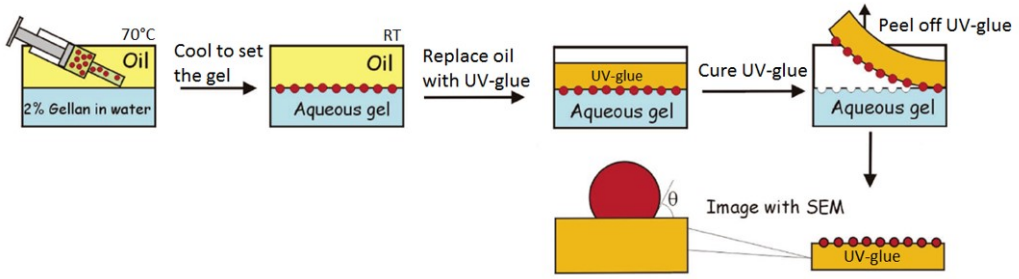

Figure 2.9: Schematic overview of an adapted version of the gel trapping technique GTT by Cayre and Paunov.[54] The particles are trapped after cooling down the solutions. In the adapted version is PDMS replaced by UV-glue and the temperature increased up to 70°C.

A replica of the water and oil phase is made to study the wettability of the cubic colloids. Solid particles are injected on the interface of a two phased system created at 70°C. The water phase consist of a 2% gellan solution that became a gel after cooling down to room temperature. The oil phase is removed and replaced by a PDMS phase. When the PDMS phase was dried, the "frozen" oil layer was peeled off and prepared for further analysis. In particular, with scanning electron microscopy (SEM) the "frozen" hematite cubes-laden interfaces are imaged.[54] In the adapted version of figure 2.9 is PDMS changed in UV-glue and a heating temperature of 70°C was used. The advantage of UV-glue is the quick and easy application and can hypothetically cause influences on the adsorption of the particles at the oil-water interface.

Before the SEM measurements, the sample must be coated with a ultra thin layer of a heavy metal. SEM is specifically intended for analyzing solid specimens that are scanned by a focused beam of high energy electrons to produce multiple signals at the surface. These signals, resulted from the sample, undergo interactions with the incoming electron beam. The elastic and inelastic scattering interactions are converted into images or other quantitative information of the sample and give more information about the cubic particle properties i.e. chemical composition, external morphology and orientation of the solid particles at the liquid-liquid interface.[49,50]

3 Experimental Section - Colloidal Cubes

In this chapter, the synthesis of different cubes is described and the corresponding methodology is explained. First the synthesis of hematite cubes with a silica coating is described, followed by the synthesis of copper oxide cubes and the synthesis of hollow silica cubes.

3.1 Hematite cubes

3.1.1 Materials

Iron(III)chloride hexahydrate (puriss, p.a., Reag. Ph. Eur., ≥99%), polyvinylpyrrolidone (PVP, 40,000 kg/mol), tetramethylammonium hydroxide solution (TMAH) 25% in H_2O, tetraethyl orthosilicate (TEOS, ≥99%), rhodamine B isothiocyanate (mixed isomers) and 3-aminopropyltriethoxysilane (APS, ≥99%) were purchased form Sigma-Aldrich (Merck). Sodium hydroxide pellets (99%) and ethanol (ACS, ISO, Reag. Ph. Eur.) were obtained from Emsure. All the chemicals were used for the syntheses as received and water was used after deionisation through a Milli-pore filter by a Milli-Q system (18.2 mΩ.cm at 20°C).[14,18]

3.1.2 Synthesis of hematite cubes

The gel-sol method was discovered by T. Sugimoto to obtain monodisperse cubic hematite particles with a yield of almost 100%.[55] Solid hematite particles could be synthesised in a variety of shapes but in this study the focus was solely on the synthesis of cubic hematite. The following two aqueous solutions prepared for this reaction were an aqueous iron(III)chloride solution, 2M $FeCl_3 \cdot 6\,H_2O$ in 100 mL of H_2O and an aqueous sodium hydroxide solution, 5M NaOH in 100 mL of H_2O. While stirring the iron(III)chloride solution in a 250 mL Pyrex bottle, a fully dissolved NaOH solution was added in approximately 15-20 seconds. The gelatinous solution reacted for ten minutes whereafter the reaction bottle was placed in an oven with a temperature of 100 °C under undisturbed conditions for 8 days. Finally, the formed particles were washed three times by centrifugation and redispersed with 200 mL of H_2O in an ultrasonic bath.[14,18]

Table 3.1: Required quantities of the chemicals for the synthesis of hematite cubes followed by the syntheses of the silica coating and the hollow silica cubes.

Required quantities of the chemicals used for syntheses.			
Chemical name	Chemical formula	Quantity	Solvent (mL)
Synthesis of hematite cubes			
iron(III)chloride solution	$FeCl_3 \cdot 6\,H_2O$	0.2 mol	100
sodium hydroxide solution	NaOH	0.5 mol	100
$Fe_2O_3 + SiO_2$			
Rhodamine-B isothiocyanate	$C_{29}H_{30}ClN_3O_3S$	0.258 mmol	5
3-aminopropyltriethoxysilane	$C_9H_{23}NO_3Si$	3.61 mmol	5
Polyvinylpyrrolidone	$(C_6H_9NO)n$	5.25 gram	150
Hematite dispersion (5 wt%)	Fe_2O_3	20 mL	
Tetramethylammonium hydroxide solution (1 wt%)	$C_4H_{13}NO$	10 mL	66 mL
Ethanol	C_2H_5OH	380 mL	
Tetraethyl orthosilicate	$SiC_8H_{20}O_4$	10 mL	10
Hollow SiO_2			
hydrochloric acid	HCl	0.8 mol	100

3.1.3 Synthesis of silica coated particles

The synthesised hematite cubes, according to the method in paragraph 3.1.2, were used for silica coating following the synthesis method of Stöber.[48] Before the silica layer could be formed around the particles, a favorable requirement to reduce aggregation during the coating was to stabilise the cubical particles with adsorbed polyvinylpyrrolidone (PVP). For a dyed silica coating allowing to visualise the cubic particles with fluorescence and confocal microscopy, 0.258 mmol of rhodamine-B isothiocyanate and 3.61 mmol of APS were dissolved in 10 mL of ethanol. The pink-dyed solution was stirred overnight in a dark room and stored in a refrigerator. The dispersed solution with 20 mL (5 wt%) of the cubic hematite particle and 5.25 g of PVP in 150 mL of H_2O was placed in a sonicate bath for 20 min after which the dispersion was stirred overnight with a magnitic strirrer.[18,19] The excess of PVP was washed away with 20 mL of ethanol and centrifuged for 20 min at 1500 rpm for two times. The solution was added to a two-necked 1 L round bottom flask, followed by 380 mL of ethanol, 66 mL of H_2O and 10 mL of TMAH (1 wt% aqueous solution). Under mechanic stirring and sonication, a TEOS solution (10 mL of TEOS in 10 mL of ethanol) and 4 mL of the dye solution were added dropwise by a Gylson peristaltic pump with a silicone tubing diameter of 1.0 mm at 4 rpm within 45 minutes. Subsequently, stirring and sonication were set for 2 hours whereafter the reaction was stirred overnight for more than 12 hours. The hematite cubes with a silica coating were washed and centrifuged with 300 mL of ethanol and redispersed for three times at 3500 rpm for 15 minutes.[18,19]

3.1.4 Synthesis of hollow silica cubes

The silica coated nanocubes as prepared in section 3.1.3 were used to dissolve the hematite core to synthesis hollow silica cubes. While stirring, hydrochloric acid was added to the hematite dispersion till an acid solution of 8M was obtained. After reacting for 24 hours the hematite core was dissolved when the solution colour turned from a dark red into a bright orange/yellow solution. If the hematite was not completely dissolved hydrochloric acid was added again as described above. At the end, the hollow silica cubes were washed with water and stored in ethanol in order to prevent the silica from dissolving.[35]

3.2 Copper oxide cubes

3.2.1 Materials

Copper(II)acetylacetonate (97%), 1,5-pentanediol (purum, $\geq$ 97.0%), polyvinylpyrrolidone (55,000 kg/mol), tetramethylammonium hydroxide solution (TMAH) 25% in H_2O, tetraethyl orthosilicate (TEOS, $\geq$ 99%) and rhodamine B isothiocyanate (mixed isomers) were obtained form Sigma-Aldrich (Merck). Acetone (practical grade) was purchased from interchema. The chemicals, ethanol (ACS, ISO, Reag. Ph. Eur.), nitric acid 65% in H_2O were purchased from Emsure. All the chemical products were used as obtained. The water used for experiments was deionised through a Milli-pore filter by a Milli-Q system (18.2 mΩ.cm at 20°C).[35]

Table 3.2: Required quantities of the chemicals for the synthesis of copper oxide cubes followed by the syntheses of the silica coating and the hollow silica cubes.

Required quantities of the chemicals used for syntheses.			
Chemical name	Chemical formula	Quantity	Solvent (mL)
Synthesis of Cu_2O cubes			
1,5-pentanediol	$C_5H_{12}O_2$	44.75 gram	
polyvinylpyrrolidone	$(C_6H_9NO)n$	5.3 gram	
copper acatylacetonate	$Cu(acac)_2$	1.04 gram	
polyvinylpyrrolidone	$(C_6H_9NO)n$	15 gram	0.2
Cu_2O + SiO2			
Polyvinylpyrrolidone	$(C_6H_9NO)n$	2.5 gram	20
Copper oxide dispersion (16 w/v%)	Cu_2O	800 mgr	
Tetramethylammonium hydroxide solution (1 wt%)	$C_4H_{13}NO$	5.35 mL	30
Ethanol	C_2H_5OH	90 mL	
Tetraethyl orthosilicate	$SiC_8H_{20}O_4$	3.3 mL	10
Hollow SiO_2			
hydrochloric acid	HCl	3 mmol	0.5
nitric acid	HNO_3	3 mmol	0.5

3.2.2 Synthesis of copper oxide cubes

An adapted version of the copper oxide synthesis from Park et al. (2009) was used for the formation of smaller cubic particles.[44] In a 250 mL three-neck round bottom flask with 44.75 g of 1,5-pentanediol was 5.3 g of polyvinylpyrrolidone dissolved while stirring with a magnetic stirrer. The reaction mixture was heated to a temperature of 100 °C using an oil bath. The mixture was heated and degassed until no more gas formation was observed after which the reaction was heated up to 195 °C. In the meantime 1.04 g of copper acatylacetonate ($Cu(acac)_2$) was suspended in 15.0 g of 1,5-pentanediol and 0.20 mL of H_2O by shaking and agitated in a sonication bath. This suspension was added in a dropping funnel where it was degassed under vacuum and flushed with nitrogen flow. As the reaction mixture reached the required temperature, the entire $Cu(acac)_2$ suspension was added through the dropping funnel in a couple of seconds. The heating was continued and after a reaction time of 20 min the synthesis was stopped. After cooling down to room temperature the particles were washed by centrifugation, one time with 200 mL of acetone and again washed for two times with 200 mL of ethanol. Finally, the copper oxide cubes were redispersed in 20 mL of ethanol.[35]

3.2.3 Synthesis of silica coated particles

The silica coating with TEOS around the cubic particles is based on the principles of the Stöber synthesis.[48] The copper oxide cubes (800 mg, 16 w/v% Cu_2O) from section 3.2.2 were added to a two-necked 500 mL round bottom flask, followed by 90 mL of ethanol, 30 mL of H_2O and 5,35 mL of TMAH (1 wt% aqueous solution). Under mechanic stirring and sonication, a TEOS solution (3.3 mL of TEOS in 10 mL of ethanol) was added dropwise by a Gylson peristaltic pump with a silicone tubing diameter of 1.0 mm at 2 rpm. The same fluorescence dye solution of paragraph 3.1.3 was used for a dyed silica coating. Finally a mixture of 2.5 g PVP in 20 mL ethanol was added to the reaction. Subsequently, stirring and sonication were set for two hours whereafter the reaction was stirred overnight for more than 12 hours. The copperoxide particles coated with silica were washed and centrifuged with 200 mL of ethanol and redispersed in 20 mL of ethanol for three times.[18,19,35]

3.2.4 Synthesis of hollow silica cubes

The silica coated nanocubes from section 3.2.3 were used to synthesise the hollow silica cubes. First, they were dispersed in 30 mL of H_2O followed by the addition of 0.5 mL of a 6M hydrochloric acid solution and 0.5 mL of a 6M nitric acid solution. The cubic despersion was heated up for one hour to a temperature of 95 °C while stirring. These steps were repeated one time in comparison with the article to completely dissolve the copper oxide core and not affect the dyed silica coating.[35]

3.3 Characterisation

The experimental part of the characterisation techniques are described in this paragraph. The synthesised particles were visualised by optical microscopy, fluorescence microscopy and transmission electron microscopy to study their shape and size.

3.3.1 Optical and fluorescence microscopy

A diluted particle dispersion of 1.0 mL was made of one droplet of the original sample dispersion. A single droplet of the diluted dispersion was applied between two glass slides with both a thickness of 1.5 mm and placed onto the stage of the microscope. The particles were imaged with an inverted optical microscope from Nikon. The Nikon ECLIPSE Ti-E with a TI-PS100W Power Supply, a TI-S-CON Motorised stage controller, and a TI-DH Dia Pillar Illuminator 100W was used. The objective lenses that were used for imaging the emulsions had a magnification of 10x, 40x and 100x (oil immersion). For the oil immersion objective, Nikon immersion oil Type A (nd=1.515) was applied onto the lens before use. For fluoresecence imaging, an Epi-fluorescence Illuminator, C-HGFI Intensilight was used in combination with the microscope. The sample preparations and other settings were similar for fluorescence microscopy.

3.3.2 Transmission electron microscopy

A single drop of a particle sample dispersion was diluted with 1.0 mL of H_2O. One droplet of this dispersed dilution was placed on a carbon coated copper grid and dried for one hour underneath a heating lamp. The synthesised cubes were imaged using high resolution transmission electron microscopy (TEM). Alternately, the following two TEMs were used, a Philips FEI Tecnai 10 operated at 100 kV using an analySIS MegaView II CCD TEM-camara for making images and a Philips FEI Tecnai 12 operated at 120 kV using an analySIS MegaView II CCD camara or a Tietz CCD camera. The colloidal particle size, shell thickness and m-value were determined by analysing the TEM-images using ImageJ.

4 Experimental Section - Cubic-Stabilised Emulsions

This experimental section presents the materials and methods needed for the formation of Pickering emulsions. The cubical colloids used for the stabilisation of the emulsion and the aqueous and oil phases are discussed.

4.1 Materials

Gellan gum powder was obtained from Alfa Aesar and ethoxylated trimethylolporpane triacrylate (ETPTA) was supplied by Sartomer. Decane ($\geq$ 99% in water), rhodamine B (dye content $\approx$ 95%) and fluorescein isothiocyanate ($\geq$ 90%) were supplied from Sigma-Aldrich (Merck) and the optical adhesive UV-glue (NOA81) was purchased from Norland. Ethanol (ACS, ISO, Reag. Ph. Eur.) was obtained from Emsure. The chemicals were used for the syntheses as received and water used in the experiments was deionised by a Milli-Q system with the following conditions, 18.2 mΩ.cm at 20°C.[14]

4.2 Cubic hematite emulsions

The formation of the Pickering emulsions is based on the procedure of de Folter.[?] The solid particles used for the the emulsions were cubic hematite particles synthesised according Section 3.1.2. Different batches of the synthesised particles are described in Table 5.1, HM007, HM004 and HMD6. The pH of the water phase was measured with a Hanna Instrument pH Meter (PH 210 Microprocessor AS-IS U). For creating the Pickering emulsion, decane as oil phase and water without any additives were used. HM004 hematite particles in a 13.6% dispersion were kept in a ultrasonic bath for 30-60 min to provide particle aggregation and support honogenisation. A glass vial of 5 mL was filled with the aqueous dispersion of hematite cubes with a known concentration and filled with H_2O to a volume of 2 mL. Then, 2 mL of decane was added to the vial whereafter 5 minutes of intensive shaking by hand was started to form emulsions including hematite.[14]

Besides using hematite cubes for the Pickering emulsions, the hollow silica cubes from the the hematite synthesis as described in Section 3.1.4 were used. For these emulsions the same particle weight, oil and water phase and the same vials were used as explained earlier. Hollow silica cubes with a size of 880 nm $\pm$ 35 nm were selected as mentioned in Table 5.1 for the experiments. In the same way sonicated to have a well homogenised dispersion. The silica particles dispersed in ethanol were washed by centrifugation and redispersed in ETPTA. The dispersion of hollow silica cubes had

a volume fraction of 1.5 v% in ETPTA. Two types of emulsions were made with the ETPTA cubic dispersion, one which contained 50 µL of the particle dispersion and one where 2 mL of the dispersion was added. To form the emulsions, 2 mL of H_2O was added to both vials including the ETPTA dispersions. The vials were manual shaken for at least 5 minutes for the formation of emulsions.[14]

4.3 Emulsions from copper oxide cubes

Copper oxide cubes, as synthesised in Section 3.2.2, were coated with a silica layer as mentioned in Section 3.2.3. Then, the Cu_2O core was dissolved which is described in Section 3.2.4, to lower the mass of the cubic particle because the core had a relative high mass. The Pickering emulsions were made with the same volume fraction which was 1.5 v% of hollow silica cubes in ETPTA. Two different emulsions were made, one vial with 50 µL of silica cubes in ETPTA and one vial with 2 mL of the cubic dispersion. Finally, the two liquids were intensively shaken by hand for the formation of the preferred hollow silica Pickering emulsions.[14]

4.4 Characterisation

The procedure for the characterisation techniques are described in this subsection. The Pickering emulsions were studied by optical microscopy and confocal microscopy. The orientation of the hematite particles at the oil-water interface was studied by scanning electron microscopy.

4.4.1 Optical microscopy

The emulsions samples were imaged with an inverted optical microscope from Nikon. The Nikon ECLIPSE Ti-E with a TI-PS100W Power Supply, a TI-S-CON Motorised stage controller, and a TI-DH Dia Pillar Illuminator 100W was used. The objective lenses that were used for imaging the emulsions had a magnification of 10x, 40x and 100x (oil immersion). For the oil immersion objective, Nikon immersion oil Type A (nd=1.515) was applied onto the lens before use. The emulsion sample was applied between two glass slides with both a thickness of 1.5 mm and placed onto the stage of the microscope.

4.4.2 Laser scanning confocal microscopy

Pickering emulsions, formed according paragraph 4.3 and 4.2, were used as they were created and the sample was analysed with laser scanning confocal microscopy, Zeiss Pascal Live. The samples were excited at 543 nm with a HeNe laser (Newport) and emission was measured between 570 and 650 nm. Pictures were made with an air objective with a magnification of 10x and a numerical aperture (NA) of 0.3 (Zeiss EC “Plan Neofluar”).

4.4.3 Scanning electron microscopy

In the theoretical background, the theory of the gel trapping technique is described where figure 2.9 is an adapted version of the literature. Cayre and Paunov used polydimethylsiloxane (PDMS) as replica of the oil phase and suggest a heating temperature of 50°C.[54] In this study, the PDMS was replaced by UV-glue and the heating temperature was increased to 70°C. This was done due to the availability and the beneficial drying time of the UV-glue related to PDMS.

In a 100 mL beaker, 2 wt% gellan was added in 20 mL of water and heated up to 70°C while stirring. Thereafter, all the materials were placed into the oven at 70°C including a petri dish, a glassy vial with the cubic particle 1:1 water/ethanol suspension and the beakers, one with the gellan solution and one with 20 mL of decane. After about 15 min, when everything has reached the desired temperature, the same amount of decane was slowly added to the aqueous solution to create an oil-water interface. With a syringe the colloidal suspension was injected close to the water-oil layer so the cubic particles were adsorbed at the interface. When the mixture was cooled down to room temperature the aqueous phase became a solid gel. Then, the decane was replaced by UV-glue for counterfeiting the oil phase because the solid particles were "trapped" into the layer of gel. The sample was placed underneath UV-light for drying and completely curing of the UV-glue layer. When the UV-layer was ready, the gel-layer was peeled off and the particles were glued to the counterfeit "oil phase". The SEM that was used for imaging the particles is a Phenom ProX desktop SEM operated at a voltage of 10 kV. The detector was a backscatter electron detector (BSD) for taking highly bright pictures of the sample.

5 Results and discussion

The results of this research are presented and discussed in this chapter. First, the synthesised hematite cubes are presented followed by the silica coating and the hollow hematite cubic particles. Thereafter, the results of the copper oxide cubes, the coated Cu_2O and the hollow Cu_2O cubes are illustrated and discussed. At the end, the formed Pickering emulsions are presented.

5.1 Hematite cubes and hollow silica cubes

Various batches of hematite cubes were synthesised and had a large variety of synthesised particles. Three batches were selected to use for this study for the Pickering emulsions. These three were selected for their shape, size of the edge length and low size polydispersity of the particles. Around one hundred individual cubic particles were used to calculate the m-value, size and the polydispersity of the hematite cubes from TEM-images. These values for the selected cubes are presented in table 5.1. The average cubic edge length had a size range between 772 nm and 1154 nm. Typical TEM-images from the hematite particles HM004 are presented in figure 5.1a and 5.1b. The synthesised hematite cubes were coated with silica and the same parameters, the size of the edge length, m-value and polydispersity were measured. An extra parameter, the shell thickness of the silica coating was calculated and is shown in table 5.1. The core of the silica coated hematite cubes was dissolved with hydrochloric acid and the hollow cubes with a remaining thickness of 54 nm are pictured in figure 5.2. As soon as the particles were coated with a silica layer the m-value of the nanocubes decreased which is observed from TEM images in figure 5.1a + 5.1b and figure 5.2. The average m-value of the hematite cubes was 3.24 and the hollow nanocubes had an average m-value of 2.95 due to the silica coating that considerably rounds the corners. By assessing these results, it was shown that the coating with silica had a large influence on the m-value of the cubes. Comparing the m-values of the hematite cubes (3.24) with the hollow cubes (2.95), the application of the silica layer modified the particle by a decrease in the m-value which was expected according to the literature.[19]

The synthesis of hematite cubes was simple to reproduce. However, the resulting particles were not perfectly cubic for every synthesis. It is known for hematite particles that their shape tends to be more rugby ball than cubic.[35,19,56] Some batches were negatively exposed to air during the reaction which affected the formation of hematite cubes. While reacting with oxygen, intermediate or side reaction occurred instead of a successful reaction. This example was shown in figure 5.3 where the formation of nanowires occurred instead of colloidal cubes.[57] According Jiang et al. (2013), this product corresponded to the goethite, $\alpha-$FeOOH, structure. These nanowires were

Table 5.1: Properties of bare and silica coated hematite cubes and hollow hematite cubes. Where $< T_{SiO_2} >$ described the thickness of the coated silica layer.

Properties of hematite cubic particles				
Name	<L> (nm)	m-value	Polydispersity (%)	$< T_{SiO_2} >$ (nm)
Fe_2O_3				
HM004	772	3.24	7.76	-
HM007	1039	3.26	4.67	-
HMD6	1453		5.8	-
$Fe_2O_3 + SiO_2$				
HM004.SDS	880	2.95	4.02	54
HM007.2SDS	1154	2.68	4.39	58
Hollow SiO_2				
HM004.HS	880	2.95	4.02	54
HM007.2HD	-	-	-	-

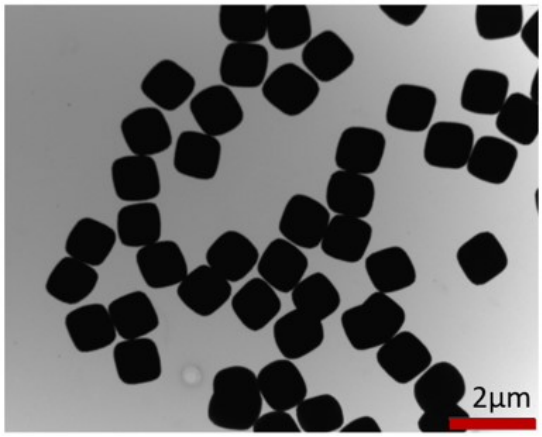

(a) Synthesised hematite cubes

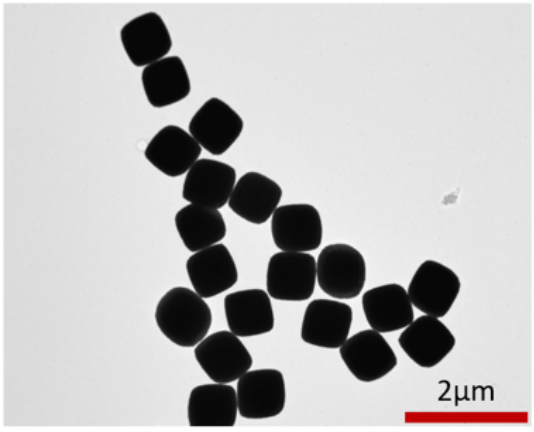

(b) The same batch of cubic hematite particles

Figure 5.1: Transmission electron microscopy (TEM) images of hematite cubic particles prepared according section 3.1 with an edge length of 772 nm ± 60 nm and an m-value of 3.24.

probably formed because there was an instability of the Fe(III)-ion caused by desorption and partial escape of the Fe(II)-ion into the aqueous phase. As a result, the fast reversible reduction and oxidation processes facilitated the growth of the goethite $\alpha-$FeOOH nanowires.[57,58]

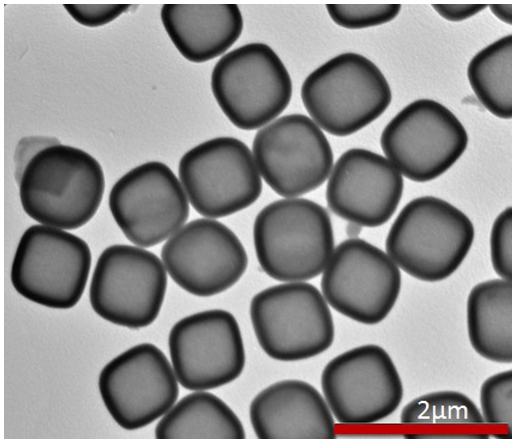

Figure 5.2: TEM-image of hollow silica cubes synthesised from the cubic hematite particles from figure 5.1a and 5.1b. The particles have a mean edge length of 880 nm ± 35 nm with a shell thickness of roughly 54 nm.

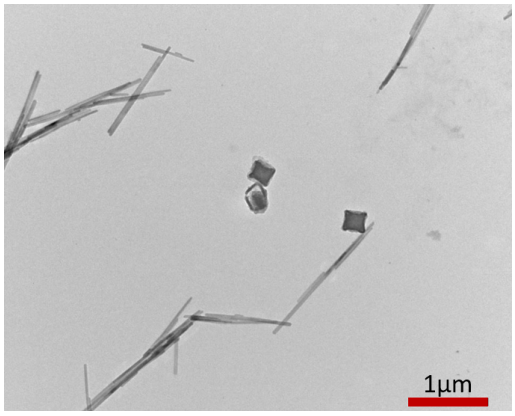

Figure 5.3: Goethite (α-FeOOH) nanowires grown as an intermediate during the synthesis of hematite cubes.

5.2 Copper oxide cubes and hollow silica cubes

An adapted version of the cubic Cu_2O synthesis of Park et al. (2009) is rewritten by Dekker et al. (*in preparation*) which gave the synthesis an upgrade to reproduce cubes with an increasing yield.[35,44] The temperature must be very carefully regulated at all times and a lower reaction temperature of 190°C-200°C was used instead of the published temperature of 240°C.[35,44] A disperse mixture of copper(II)acetylacetonate ($Cu(acac)_2$) in 1,5-pentanediol was facilitated and alternated by using a vortex and sonication. By prevention in advance, big aggregates of $Cu(acac)_2$ were not formed which made the addition by a dropping funnel more feasible. Cubic shaped particles were formed but no conclusive data on the impurity of the particles could been acquired.

Cubic particles in figure 5.4a, 5.4b and 5.4c were analysed according to section 3.3 by transmission electron microscopy. The properties of various copper oxide particles are listed in table 5.2. Cubic copper oxide particle size, synthesised for this study, ranged between 57 nm and 72 nm, which was significantly smaller related to hematite cubes. The bare copper oxide cubes (figure 5.4a) were coated with silica (figure 5.4b). The thickness of the silica coating around the copper oxide cubes was varying during

several synthesis for a constant quantity of TEOS. Nevertheless, more factors played a role during the synthesis. The coating thickness could be affected by the reaction temperature or the amount of added water during the reaction. Therefore, it was challenging to find the optimal quantity of TEOS for a suitable layer of silica. The layer was either too thick so the cubic particles were becoming more spherical or too thin so the hollow silica cubes collapsed when the core was dissolved. For additional studies, it could be interesting to investigate the ratio between the quantity of TEOS and the shell thickness whereby external factors (temperature and added water) could be excluded. The colloidal particles in figure 5.4a had an average edge length of 72 nm ± 12 nm and an m-value of 5.49. This higher m-value with respect to hematite cubes of figure 5.1a and 5.1b means that Cu_2O cubes reached a more perfect cubic shape than a superball shape. The cubes of figure 5.4b were used for the silica coating after which their size increased with a shell thickness of 33 nm and their m-value decreased to 2.65. The large reduction in m-value was caused by the silica coating that flattens the cubes' corners. This might have an effect during the particles adsorption at the interface while forming an emulsion. It might causes a change in the contact angle when the particles were adsorbed between the oil and water phase. The corners of the copper oxide cubes had increased rounded corners and the cubes lost their flat edge length with a constant contact angle when the cubicity approached towards a superball shape after the silica coating.

Table 5.2: Properties of bare and silica coated copper oxide cubes and hollow copper oxide cubes

Properties of copper oxide cubic particles				
Name	<L> (nm)	*m*-value	Polydispersity (%)	$< T_{SiO_2} >$ (nm)
Cu_2O				
HM010	65.4	8.01	15	-
HM011	72	5.49	17	-
HM014	57.6	9.55	11	-
$Cu_2O + SiO_2$				
HM011.SDS	138	2.65	14	33
Hollow SiO_2				
HM011.HD	131	2.66	12	30

The next step of the synthesis was to hollow the silica coated copper oxide cubes as described in section 3.2.4. The silica coated copper oxide particles from figure 5.4b were used to disperse in 30 mL of an aqueous solution with 0.5 mL of a 6M hydrochloric acid solution and 0.5 mL of a 6M nitric acid solution. The particles became hollow in the acid created conditions and were shown in figure 5.4c. A decrease in shell thickness was measured which could be explained by dissolution of the copper oxide core using strong acids. This solution of strong acids could have caused the porous silica to shrink or dissolve several nanometers without a change in m-value. These hollow silica particles used for orientation studies and for stabilisation of the Pickering emulsions had a size of 131 nm ± 16 nm and an m-value of 2.66. As described earlier, particles with an m-value of around 3 were becoming cubical and when the m-value increases the particles

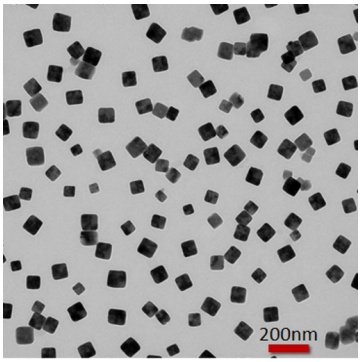

(a) TEM-image of cubic copper oxide, m-value of 5.49.

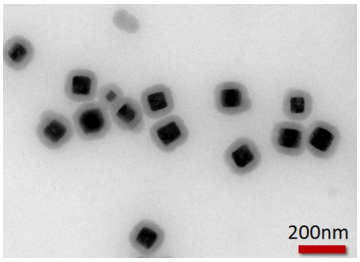

(b) A TEM-image of Cu_2O cubes coated with silica, m-value of 2.65.

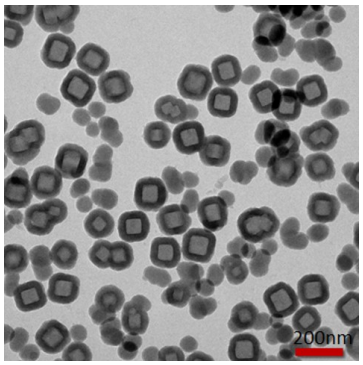

(c) Hollow silica cubes synthesised from the cubes of figure 5.4b, m-value of 2.66.

Figure 5.4: TEM-images of cubic Cu_2O particles prepared according Section 3.2 (a) bare copper oxide particles with an edge length of 72 nm ± 12 nm (b) the same synthesised Cu_2O cubes coated with silica which have a shell thickness of 33 nm. (c) Cubic hollow silica particles prepared according section 3.2.4 with the particles from image b which have an edge length of 131 nm ± 16 nm. and a shell thickness of 30 nm

approach a perfectly shaped cube.[19,35,36] In table 5.2, the synthesised batch of copper oxide nanocubes had an m-value of 9.55, illustrated in figure 5.5. The colloidal particles had an m-value of 9.55 which resulted in sharp angular corners and had a side length of 57.6 nm ± 6.3 nm. For further investigations, it will be interesting to coat this batch of cubes (HM14) and make Pickering emulsions from these Cu_2O cubes with a high m-value to study their interface orientation and emulsion stability.

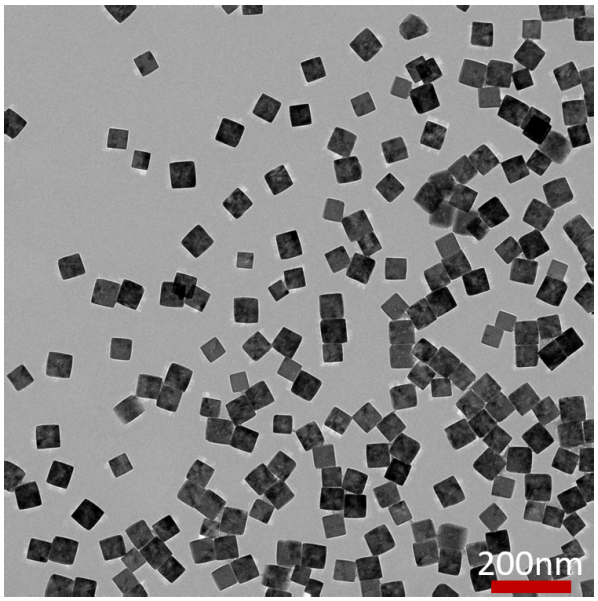

Figure 5.5: Transmission electron microscopy image of copper oxide particles prepared according Section 3.2.2 with an edge length of 57.6 nm ± 6.3 nm and had an m-value of 9.55.

5.3 Fluorescence microscopy

Hematite particles, synthesised according section 3.1.3, were imaged by fluorescence microscopy. The microscopic pictures in figure 5.6a and 5.6b were hematite cubes with a dyed silica coating by using a 40x optical zoom lens. The average size of the bare hematite particles was 1039 nm ± 48.5 nm with an m-value of 3.26. The size length increased to 1154 nm ± 50.7 nm with a reduced m-value of 2.68 after coating the colloidal cubes with silica. In the picture of figure 5.6b, it is clearly visible that the silica around the particles was dyed with a rhodamine B isothiocyanate silica coating due to the excitation wavelength of 510 nm (green colour). This picture could be compared with figure 5.6a for more clarification of the coated hematite cubes. The coated particles could be used for orientation studies to see how the particles were orientated at the oil-water interface of Pickering emulsions.

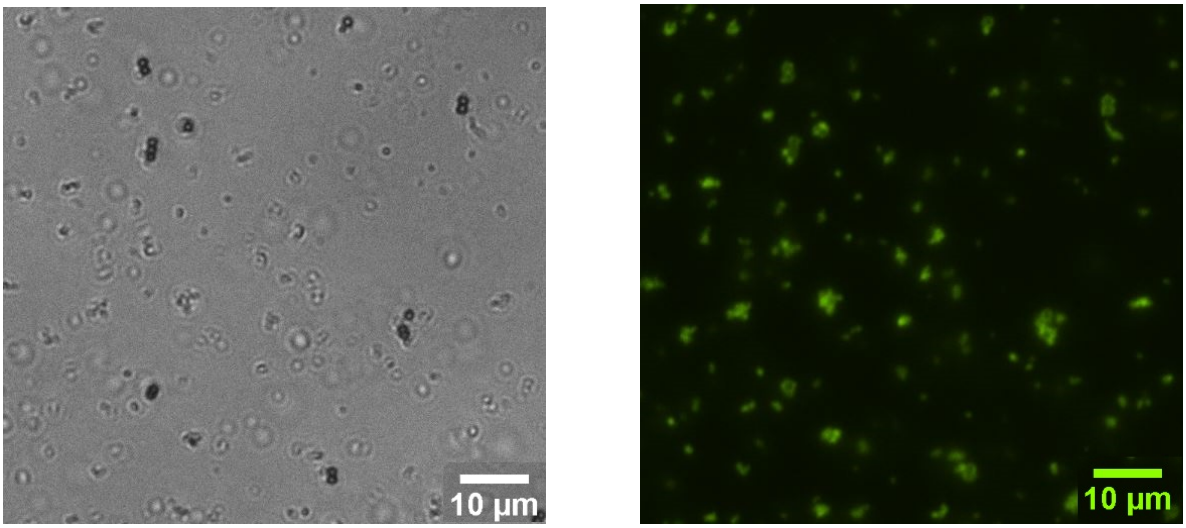

(a) Hematite cubes covered with a dyed silica coating

(b) Same image of hematite cubes covered with a dyed silica coating

Figure 5.6: Microscope images of hematite coated cubes with a size length of 1154 nm ± 50.7 nm, an m-value of 2.68 and a coating thickness of roughly 58 nm. In image (a), a regular microscope image was shown and in image (b) a laser was used to visualise the dyed silica coating around the Fe_2O_3 cubes

The dye in the silica was applied to make the particles traceable and visible to study the orientation of hollow silica cubes when they were adsorbed at the oil-water interface. The rhodamine B isothiocyanate adhered well in the silica layer and had no noticeable influence on the orientation or hydrophobicity or hydrophilicity. Therefore, this uncertainty was neglected during this study. The particles were washed several times to remove the access of silica aggregates. The procedure of section 3.1.3 turns out to be a good method, but regulating the thickness of the silica layer stays difficult.

5.4 Scanning electron microscopy

The three phase contact angle of the hematite, Fe_2O_3 particles was measured as described in section 2.3.4 and 4.4.3. Instead of using PDMS, UV-glue was used for replicating the oil phase.[54] The top view of the SEM-images in figure 5.7a and 5.7b gave a good first result of how solid hematite particles were dispersed at the interface in Pickering emulsions. The field of vision in the picture was from the water phase onto the imitated oil phase, the UV-glue. In figure 5.7a, it was observed that the oil-water interface was covered with a close packed, [100]-orientated monolayer of cubes. The gel trapping technique was to a certain extent a reliable method for the study of interfacial behaviour such as the contact angle of the cubical particles. The results showed that the cubic particles were laying on top of the "oil phase" instead of partly immersed in the water phase. As expected, the particles were preferring the aqueous phase and showed for single particles a thermodynamically favourable parallel orientation. From images 5.8a and 5.8b, it could be concluded that cubic hematite was preferentially exposed to the water phase. The method was easy to implement and a quick feasible way to obtain information of the particles' orientation. Unexpected was that the colloidal cubes were not immersed into the "oil phase". This could be explained by the addition of gellan to the water phase and by substituting the PDMS with UV-glue. This could have an influence on the adsorption and the orientation of the hematite particles at the interface.[54,21] From the experiments and the scanning electron microscope images, it was impossible to calculate the contact angle as described in section 2.3.4. The ratio between the particle length inside the water and the oil phase could not be analysed due to the fact that the particles were laying on top of the UV-glue. In supplementary studies, this method could be improved by following the original procedure according section 2.3.4 or the observation of the particle orientation could be done by the method of de Folter (2013) where solidified droplets were analysed.[14,54]

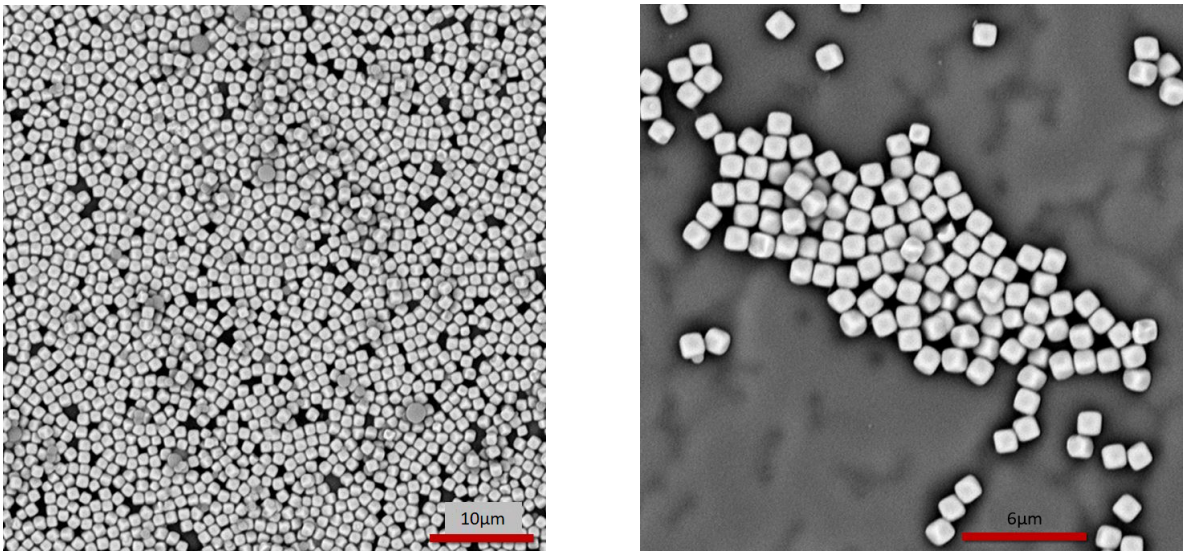

(a) SEM-image of hematite cubes

(b) Another SEM-image of Fe_2O_3 cubes

Figure 5.7: Scanning electron microscopy images of cubic Fe_2O_3 particles prepared according section 3.1 with an edge length of 772 nm ± 60 nm and m-value of 3.24.

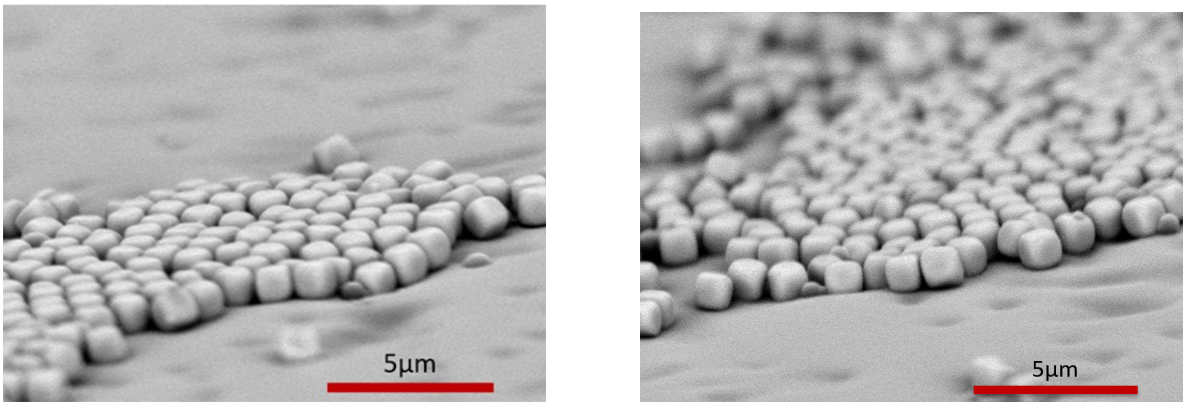

(a) SEM-image of cubic hematite (b) Another SEM-image of Fe_2O_3 cubes

Figure 5.8: SEM-images with a side view of cubic Fe_2O_3 particles prepared according section 3.1 with an edge length of 772 nm ± 60 nm and m-value of 3.24.

5.5 Pickering emulsions

After obtaining cubic hematite particles from the synthesis in section 5.1, the particles in table 5.1 were selected for the formation of Pickering emulsions (figure 5.9). These Pickering emulsions were based on water and decane and created after shaken by hand. The cubic particles migrated from the water phase to the oil-water interface wherein this adsorption ensured a preferred kinetically stable state.[5] The hematite dispersion which was directly used after the synthesis was not forming a stable Pickering emulsion. More washing, according to the experimental section, was improving the Pickering emulsion formation due to the acidity aqueous phase. With a pH-measuring device the pH of the redispersed water of the Fe_2O_3 cubes was 2.5 and after washing it two more times the pH increased to 4.6. It turned out that the initial conditions of the particles were not optimal to spontaneously form Pickering emulsions. After increasing the pH of the particle dispersion the emulsion was stable up to at least six months. Accoriding S. Fujii et al. (2006), no emulsification can occur around a pH of 2 and stable Pickering emulsions were formed around a pH above 5.6.[38] The pH of the formed Pickering emulsion was 4.6 which is lower than the literature due to emulsification with different particles. From this could be concluded that Pickering emulsions could not form at relative low pH since hematite cubes in water had a pH between 2 and 3.[36,38] The low pH, occurred after the reaction, was affected by the formed H_3O^+ during the reaction. Figure 5.9a showed a picture of both emulsions after 2 months. The pH was a crucial factor for the formation and stabilisation of the oil-in-water emulsions. In fact, to prevent coalescence of the oil droplets, the iso-electric point had to be taken into account.

The cubic hematite and the copper oxide particles were coated with silica respectively according section 3.1.3 and section 3.2.3 to vary the chemical composition of the particles. The benefit of dissolving the hematite and the copper oxide core of the cubes respectively according section 3.1.4 and 3.2.4 was to reduce the influence from gravitational forces what eventually could limit emulsion destabilisation. Besides the change in chemical composition, another advantage of the hollow cubes is the reduction in particle weight. Hollow cubes were lighter and could decrease gravitational forces, which is one of the causes of emulsion instability. These two different hollow silica

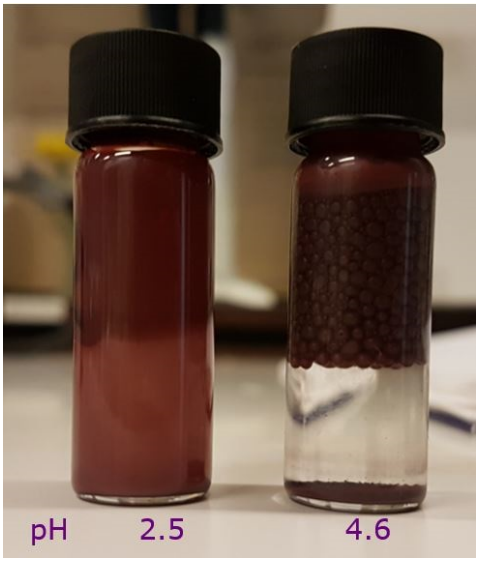

(a) Picture of a destabilised PE, pH of 2.5 and a stable PE, pH of 4.6. Both PE had a 1:1 ratio, decane:water with 4 wt% hematite cubes in water.

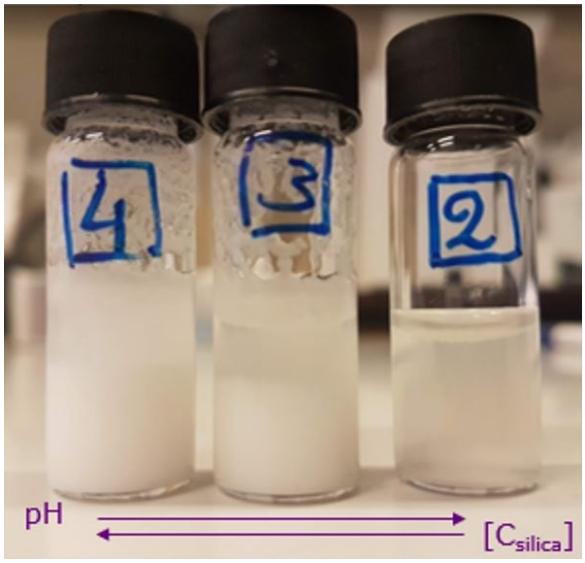

(b) Picture of stabilised PE by bigger silica cubes (880 nm ± 35 nm). The PE had a 1:1 ratio, ETPTA:water with 1.5 v/v% cubes in ETPTA.

Figure 5.9: Pickering emulsions stabilised by (a) cubic hematite particles of 1453 nm ± 84 nm and (b) hollow silica cubes with a size length of 880 nm ± 35 nm, m-value of 2.95. The emulsions had a 1:1 ratio of oil:water.

cubes from figure 5.2 and 5.4c had the same chemical composition but a different edge length. The bigger silica cubes have a length of 880 nm ± 35 nm and the length of the smaller cubic particles are 131 nm ± 16 nm. Two different Pickering emulsions were illustrated by optical microscopy images in figure 5.10a and 5.10b. The Pickering emulsions formed spontaneously after manual shaking and after reaching their kinetically stable state the emulsion was stable against coalescence. The emulsions had the same ratio of oil:water, 1:1 where the emulsions of figure 5.9a and 5.9b had a ratio respectively of decane:water and ETPTA:water. The weight percentage of particles in the emulsions in both pictures were different. The hematite cubes, in a 4 wt% colloidal dispersion, were added to the oil phase. The volume/volume concentration of the silica particles was 1.5 v/v% hollow silica cubes in ETPTA in vail number 2 and 3 and 3.0 v/v% hollow silica cubes in ETPTA in vail number 4. When the concentration of the hollow cubic particles increases, the pH would hypothetically decreased as shown in figure 5.9b. In the three emulsions, the water phase was dyed with a water soluble dye, fluorescein isothiocyanate, in order to analyse the emulsions with laser scanning confocal microscopy (LSCM). The dye was added to the water phase to increase the distinctive ability between the oil and water phase but the added dyed could had an influence on the particle orientation due to a slightly change of the water phase.

In the two optical microscopy images, figure 5.10a and 5.10b, could be seen how the oil droplets were homogenised in the water phase. In figure 5.10a the oil droplets were stabilised by hollow silica cubes synthesised, according to section 3.2.4, where the copper oxide core was dissolved. The adsorbed hollow silica nanocubes had a size of 131 nm ± 16 nm, an m-value of 2.66 and a silica shell thickness of 30 nm. The size of the oil droplets dispersed in the water phase had a diameter of approximately 16.5 µm

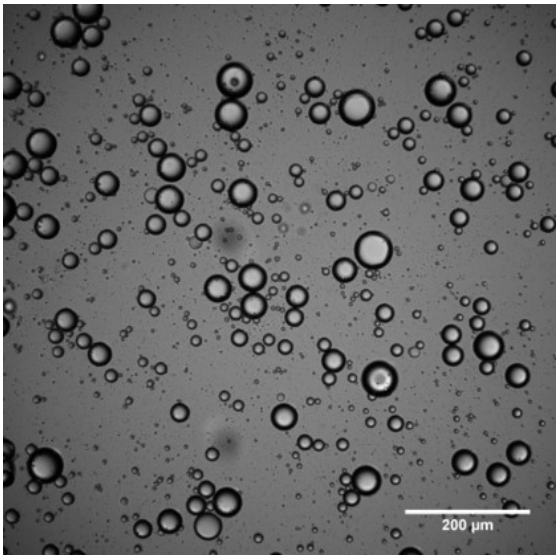

(a) Oil droplets stabilised by smaller silica cubes of 131 nm ± 16 nm in an ETPTA:water, 1:1 ratio with 1.5 v/v%.

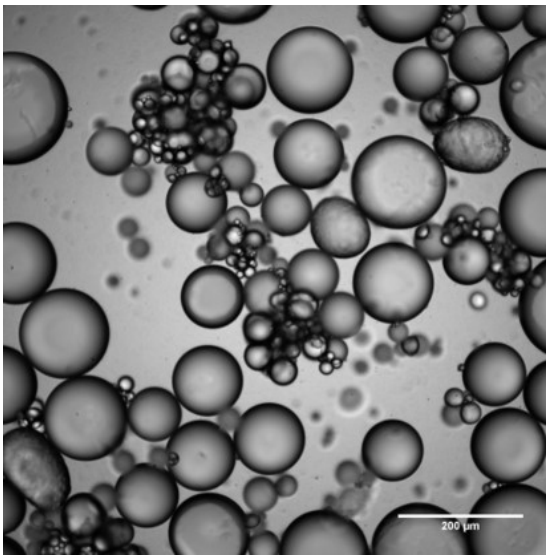

(b) Oil droplets stabilised by bigger silica cubes of 880 nm ± 35nm in an ETPTA:water, 1:1 ratio with 1.5 v/v%.

Figure 5.10: Optical microscope images of balanced o/w Pickering emulsions stabilised by hollow silica cubes, synthesised from (a) copper oxide cubes and (b) hematite cubes.

± 13.0 µm. Comparing this with figure 5.10b, it could be observed that the dispersed oil droplets in water were significant bigger by using bigger hollow silica cubes with a size length of 880 nm ± 35 nm, an m-value of 2.95 and a silica shell thickness of 54 nm. The oil droplets had an average diameter of 52.3 µm ± 43.6 µm. The volume percentage was kept the same so a difference in the amount of added hollow silica cubes was observed between the two emulsions. Further investigation could be done on the study of the correlation between the size of the hollow silica cubes and the oil droplets in the oil-in-water emulsions.

Figure 5.11 is a 100 times enlarged picture from figure 5.10b where the structured orientation of the adsorbed cubical hollow particles at the oil water interface was visible. The bigger hollow silica cubes had a size range of almost 1 micrometer and possible to image with optical microscopy. Unfortunately, the smaller hollow silica cubes were too small for the same type of images. The droplet, with a diameter of 63.7 micrometer, was stabilised by hollow silica cubes of circa 880 nm ± 35 nm, an m-value of 2.95 and a silica shell thickness of 54 nm. Finally, these optical microscopy images confirmed that this type of oil-in-water emulsion was stable against the occurrence of coalescence.

As described before, figure 5.12a and 5.12b were pictured with laser scanning confocal microscopy to study the oil droplets in the water phase. Hence, after varying the addition of oil and water, these images gave the result that phase inversion occurred with these Pickering emulsions. Both emulsions had the same conditions, the droplets were stabilised by bigger silica cubes of 880 nm ± 35 nm synthesised from the hematite reaction and had a ratio of ETPTA:water, 1:1 of 1.5v/v% particles in water. The only difference was that figure 5.12a had oil droplets in the water phase and figure 5.12b had water droplets in the oil phase. From this result, it seems that the order of addition

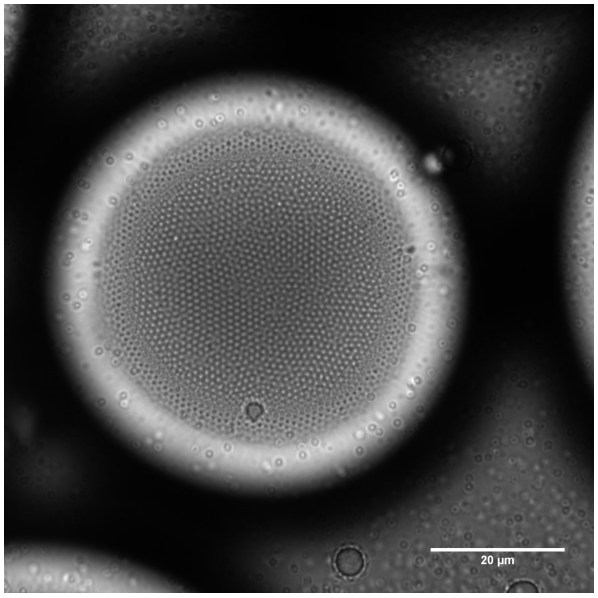

Figure 5.11: Optical microscopy image of one oil droplet in water stabilised by hollow silica cubes. This was a 100x zoomed image of an oil droplets from figure 5.10b stabilised with particles of 880 nm ± 35 nm in an ETPTA:water, 1:1 ratio with 1.5 v/v%.

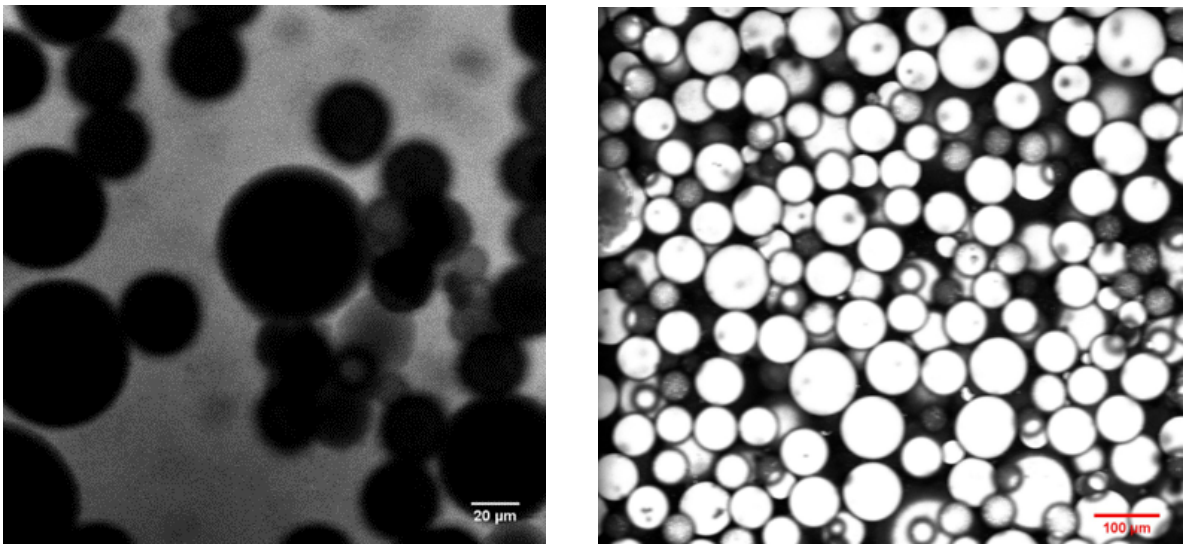

(a) Oil droplets stabilised by bigger silica cubes of 880 nm ± 35 nm.

(b) Water droplets stabilised by bigger silica cubes of 880 nm ± 35 nm.

Figure 5.12: Confocal microscope images of a balanced oil-in-water Pickering emulsion, figure 5.12a and a balanced water-in-oil Pickering emulsion, figure 5.12b. Both stabilised by hollow silica cubes synthesised from hematite cubes stabilise.

was a crucial factor. Cubical particles in water with added oil and cubical particles in oil with added water resulted respectively in w/o emulsions and in o/w emulsions. Accorrding to the literature, phase inversion is induced by changing the volume fraction of the dispersion. The phase inversion changes for a water-in-oil to an oil-in-water emulsion for hydrophobic silica (TEOS) and the emulsion stability reduced substantially at concentrations as the contact angles increases up to 90°.[32,59]

6 Conclusion

Colloidal cubes of different sizes and chemical compositions are synthesised and used for adsorption at the oil-water interface to form Pickering emulsions. As expected, Pickering emulsions with hematite cubes and hollow silica cubes are easily formed. The cubic hematite particles are [100] orientated in the water phase resulting in a close packed monolayer which is confirmed with the Gel Trapping Technique and scanning electron microscopy. Pickering emulsions with a pH between 4 and 7 are shown to be stable for at least 6 months, without showing coalescence or other physical instabilities. Optical microscopy images confirm for a similar solid load that smaller and larger hollow silica cubes produce respectively smaller and bigger oil droplets. Laser scanning confocal microscopy further supports the formation of oil-in-water emulsions for both types of hollow silica cubes. A crucial step in the preparation of the Pickering emulsion is shown to be the order of addition. When hollow silica cubic particles are dispersed in water and subsequently oil is added, a water-in-oil emulsion is obtained. Vice versa, addition of water to cubic particles dispersed in oil cause a oil-in-water emulsion.

7 Outlook

Further investigation on Pickering emulsions is advisable in the field of optimisation of the emulsion conditions to increase the stability of the Pickering emulsions. The following recommendations for the outlook of this study are suggested;

Further research on the particle load and the surface packing can be studied to determine their influence on the stability of the emulsions. More extended research on the preferred orientations and the exact locations of the anisotropic particles adsorbed on the interface can be done to study the emulsion formations and enhance the emulsion stability. Images from laser scanning confocal microscopy showed that the order of particle addition is very important for this type of emulsions. Investigating the emulsion system and the order of addition can be interesting to determine the inversion point of the different Pickering emulsions in this research. Furthermore, the determination of the used quantity of silica and the shell thickness was complex and additional research can be carried out by investigating their consistency. Further investigations can be done to analyse the correlation between the size of the hollow silica particles and the droplet size in the oil-in-water and water-in-oil emulsions. Pickering emulsions were formed with a ratio of 1:1 (oil:water) which results to an excess of water. Additionally, it will be interesting to find the optimal ratio for the Pickering emulsions. The possible next step is to find one ratio similar for both, Pickering emulsions and conventional emulsions. Supplementary methods for squeeze flow experiments with Pickering emulsions need to be investigated, followed by measuring the differences in stability where the results of conventional emulsions are compared with Pickering emulsions. Eventually, this will give additional information necessary to answer the main goal of this study; are Pickering emulsions stabilised with cubes more stable than surfactant-stabilised emulsions.

Bibliography

[1] Claire C. Berton-Carabin and Karin Schroën. Pickering emulsions for food applications: Background, trends, and challenges. *Annual Review of Food Science and Technology*, 6(1):263–297, apr 2015.

[2] Adriana San-Miguel and Sven H. Behrens. Influence of nanoscale particle roughness on the stability of pickering emulsions. *Langmuir*, 28(33):12038–12043, aug 2012.

[3] Emanuele Vignati, Roberto Piazza, and Thomas P. Lockhart. Pickering emulsions: interfacial tension, colloidal layer morphology, and trapped-particle motion. *Langmuir*, 19(17):6650–6656, aug 2003.

[4] David J. French, Aidan T. Brown, Andrew B. Schofield, Jeff Fowler, Phil Taylor, and Paul S. Clegg. The secret life of pickering emulsions: particle exchange revealed using two colours of particle. *Scientific Reports*, 6(1), aug 2016.

[5] David Julian McClements. *Food Emulsions*. CRC Press, 2015.

[6] David Julian McClements. Emulsion design to improve the delivery of functional lipophilic components. *Annual Review of Food Science and Technology*, 1(1):241–269, apr 2010.

[7] Like Mao and Song Miao. Structuring food emulsions to improve nutrient delivery during digestion. *Food Engineering Reviews*, 7(4):439–451, jan 2015.

[8] Paul S. Clegg, Joe W. Tavacoli, and Pete J. Wilde. One-step production of multiple emulsions: microfluidic, polymer-stabilized and particle-stabilized approaches. *Soft Matter*, 12(4):998–1008, 2016.

[9] David S Home. Protein-stabilized emulsions. *Current Opinion in Colloid & Interface Science*, 1(6):752–758, dec 1996.

[10] Tharwat F. Tadros. *Emulsions*. de Gruyter Oldenbourg, 2016.

[11] M. F. Haase. *Modification of Nanoparticle Surfaces for Emulsion Stabilisation and Encapsulation of Active Molecules for Anti-Corrosive Coatings*. PhD thesis, Max Planck Institute of Colloids and Interfaces, University of Potsdam, 2011.

[12] W. Ramsden. Separation of solids in the surface-layers of solutions and 'suspensions' (observations on surface-membranes, bubbles, emulsions, and mechanical coagulation).—preliminary account. *Proceedings of the Royal Society of London*, 72(477-486):156–164, jan 1904.

[13] Spencer Umfreville Pickering. CXCVI.—emulsions. *J. Chem. Soc., Trans.*, 91(0):2001–2021, 1907.

[14] Julius W. J. de Folter, Eline M. Hutter, Sonja I. R. Castillo, Kira E. Klop, Albert P. Philipse, and Willem K. Kegel. Particle shape anisotropy in pickering emulsions: Cubes and peanuts. *Langmuir*, 30(4):955–964, sep 2013.

[15] R. Skartlien, B. Grimes, P. Meakin, J. Sjöblom, and E. Sollum. Coalescence kinetics in surfactant stabilized emulsions: Evolution equations from direct numerical simulations. *The Journal of Chemical Physics*, 137(21):214701, dec 2012.

[16] Hamed Vahabi, Wei Wang, Joseph M. Mabry, and Arun K. Kota. Coalescence-induced jumping of droplets on superomniphobic surfaces with macrotexture. *Science Advances*, 4(11):eaau3488, nov 2018.

[17] S. Arditty, C. P. Whitby, B. P. Binks, V. Schmitt, and F. Leal-Calderon. Some general features of limited coalescence in solid-stabilized emulsions. *The European Physical Journal E*, 11(3):273–281, jul 2003.

[18] Laura Rossi, Stefano Sacanna, William T. M. Irvine, Paul M. Chaikin, David J. Pine, and Albert P. Philipse. Cubic crystals from cubic colloids. *Soft Matter*, 7(9):4139–4142, 2011.

[19] Sonja I.R. Castillo, Samia Ouhajji, Sander Fokker, Ben H. Erné, Chris T.W.M. Schneijdenberg, Dominique M.E. Thies-Weesie, and Albert P. Philipse. Silica cubes with tunable coating thickness and porosity: From hematite filled silica boxes to hollow silica bubbles. *Microporous and Mesoporous Materials*, 195:75–86, sep 2014.

[20] Thriveni G. Anjali and Madivala G. Basavaraj. Shape-anisotropic colloids at interfaces. *Langmuir*, 35(1):3–20, jul 2018.

[21] Thriveni G. Anjali and Madivala G. Basavaraj. Shape-induced deformation, capillary bridging, and self-assembly of cuboids at the fluid–fluid interface. *Langmuir*, 33(3):791–801, jan 2017.

[22] J. W.J. de Folter. *Interplay between colloids and interfaces*. PhD thesis, Utrecht University, 2013.

[23] Yves Chevalier and Marie-Alexandrine Bolzinger. Emulsions stabilized with solid nanoparticles: Pickering emulsions. *Colloids and Surfaces A: Physicochemical and Engineering Aspects*, 439:23–34, dec 2013.

[24] Samuel Levine, Bruce D. Bowen, and Susan J. Partridge. Stabilization of emulsions by fine particles i. partitioning of particles between continuous phase and oil/water interface. *Colloids and Surfaces*, 38(2):325–343, jan 1989.

[25] Mark Vis, Joeri Opdam, Ingo S. J. van 't Oor, Giuseppe Soligno, René van Roij, R. Hans Tromp, and Ben H. Erné. Water-in-water emulsions stabilized by nanoplates. *ACS Macro Letters*, 4(9):965–968, sep 2015.

[26] Pyotr M Kruglyakov and Alla V Nushtayeva. Phase inversion in emulsions stabilised by solid particles. *Advances in Colloid and Interface Science*, 108-109:151–158, may 2004.

[27] Krassimir P. Velikov Peter Veenstra Annie Colin Hamid Kellay Willem K. Kegel Riande I. Dekker, Antoine Deblais and Daniel Bonn. Manuscript in preparation. 2019.

[28] Demet Guzey and D. Julian McClements. Formation, stability and properties of multilayer emulsions for application in the food industry. *Advances in Colloid and Interface Science*, 128-130:227–248, dec 2006.

[29] Nissim Garti and Chris Bisperink. Double emulsions: Progress and applications. *Current Opinion in Colloid & Interface Science*, 3(6):657–667, dec 1998.

[30] Eric Dickinson. Use of nanoparticles and microparticles in the formation and stabilization of food emulsions. *Trends in Food Science & Technology*, 24(1):4–12, mar 2012.

[31] Hildebrand J. H. Finkle P., Draper H. D. The theory of emulsification. *JACS*, 45:2780–2788, 1923.

[32] B. P. Binks and S. O. Lumsdon. Catastrophic phase inversion of water-in-oil emulsions stabilized by hydrophobic silica. *Langmuir*, 16(6):2539–2547, mar 2000.

[33] Jan Engmann, Colin Servais, and Adam S. Burbidge. Squeeze flow theory and applications to rheometry: A review. *Journal of Non-Newtonian Fluid Mechanics*, 132(1-3):1–27, dec 2005.

[34] Chris Evers. *Colloidal Self-Assembly Driven by Deformability and Near-Critical Phenomena*. PhD thesis, University Utrecht, 2016.

[35] Frans Dekker, Remco Tuinier, and Albert Philipse. Synthesis of hollow silica nanocubes with tuneable size and shape, suitable for light scattering studies. *Colloids and Interfaces*, 2(4):44, oct 2018.

[36] Janne-Mieke Meijer, Dmytro V. Byelov, Laura Rossi, Anatoly Snigirev, Irina Snigireva, Albert P. Philipse, and Andrei V. Petukhov. Self-assembly of colloidal hematite cubes: a microradian x-ray diffraction exploration of sedimentary crystals. *Soft Matter*, 9(45):10729, 2013.

[37] Mark Weller. *Inorganic Chemistry*. OUP, 2014.

[38] Syuji Fujii, Steven P. Armes, Bernard P. Binks, and Ryo Murakami. Stimulus-responsive particulate emulsifiers based on lightly cross-linked poly(4-vinylpyridine)-silica nanocomposite microgels. *Langmuir*, 22(16):6818–6825, aug 2006.

[39] P Taneja, R Chandra, R Banerjee, and P Ayyub. Structure and properties of nanocrystalline ag and cu 2 o synthesized by high pressure sputtering. *Scripta Materialia*, 44(8-9):1915–1918, may 2001.

[40] E. G. Ponyatovskii, G. E. Abrosimova, A. S. Aronin, V. I. Kulakov, I. V. Kuleshov, and V. V. Sinitsyn. Nanocrystalline cu2o prepared under high pressures. *Physics of the Solid State*, 44(5):852–856, may 2002.

[41] W.Z. Wang G.H. Wang X.S. Wang Y.J. Zhan Y.K. Liu C.L. Zheng. Synthesis and characterization of cu2o nanowires by a novel reduction route. *Adv. Mater.*, 14(1):67–69, January 2002.

[42] Linfeng Gou and Catherine J. Murphy. Solution-phase synthesis of cu2o nanocubes. *Nano Letters*, 3(2):231–234, feb 2003.

[43] H. Dong, Y.-C. Chen, and C. Feldmann. Polyol synthesis of nanoparticles: status and options regarding metals, oxides, chalcogenides, and non-metal elements. *Green Chemistry*, 17(8):4107–4132, 2015.

[44] Ji Chan Park, Jeonghan Kim, Hyuksang Kwon, and Hyunjoon Song. Gram-scale synthesis of cu2o nanocubes and subsequent oxidation to CuO hollow nanostructures for lithium-ion battery anode materials. *Advanced Materials*, 21(7):803–807, feb 2009.

[45] Liang Chen, Yu Zhang, Pengli Zhu, Fengrui Zhou, Wenjin Zeng, Daoqiang Daniel Lu, Rong Sun, and Chingping Wong. Copper salts mediated morphological transformation of cu2o from cubes to hierarchical flower-like or microspheres and their supercapacitors performances. *Scientific Reports*, 5(1), apr 2015.

[46] F FIEVET, J LAGIER, B BLIN, B BEAUDOIN, and M FIGLARZ. Homogeneous and heterogeneous nucleations in the polyol process for the preparation of micron and submicron size metal particles. *Solid State Ionics*, 32-33:198–205, feb 1989.

[47] Andrés Guerrero-Martínez, Jorge Pérez-Juste, and Luis M. Liz-Marzán. Recent progress on silica coating of nanoparticles and related nanomaterials. *Advanced Materials*, 22(11):1182–1195, mar 2010.

[48] Werner Stöber, Arthur Fink, and Ernst Bohn. Controlled growth of monodisperse silica spheres in the micron size range. *Journal of Colloid and Interface Science*, 26(1):62–69, jan 1968.

[49] Bruce Alberts. *Essential Cell Biology.* Garland Science, 2010.

[50] Anthony L. Mescher. *Junqueira's Basic Histology: Text & Atlas.* McGraw Hill, 2010.

[51] Edward W. Washburn. The dynamics of capillary flow. *Physical Review*, 17(3):273–283, mar 1921.

[52] N. Denkov, O. Velev, P. Kralchevski, I. Ivanov, H. Yoshimura, and K. Nagayama. Mechanism of formation of two-dimensional crystals from latex particles on substrates. *Langmuir*, 8(12):3183–3190, dec 1992.

[53] Z. Li, R.F. Giese, C.J. van Oss, J. Yvon, and J. Cases. The surface thermodynamic properties of talc treated with octadecylamine. *Journal of Colloid and Interface Science*, 156(2):279–284, mar 1993.

[54] Olivier J. Cayre and Vesselin N. Paunov. Contact angles of colloid silica and gold particles at air-water and oil-water interfaces determined with the gel trapping technique. *Langmuir*, 20(22):9594–9599, oct 2004.

[55] Tadao Sugimoto, Mohammad M. Khan, and Atsushi Muramatsu. Preparation of monodisperse peanut-type α-Fe_2O_3 particles from condensed ferric hydroxide gel. *Colloids and Surfaces A: Physicochemical and Engineering Aspects*, 70(2):167–169, mar 1993.

[56] Janne-Mieke Meijer, Fabian Hagemans, Laura Rossi, Dmytro V. Byelov, Sonja I.R. Castillo, Anatoly Snigirev, Irina Snigireva, Albert P. Philipse, and Andrei V. Petukhov. Self-assembly of colloidal cubes via vertical deposition. *Langmuir*, 28(20):7631–7638, may 2012.

[57] Shenghua Jiang, Min-Gyu Kim, In Young Kim, Seong-Ju Hwang, and Hor-Gil Hur. Biological synthesis of free-standing uniformed goethite nanowires by shewanella sp. HN-41. *J. Mater. Chem. A*, 1(5):1646–1650, 2013.

[58] Hua-Feng Shao, Xue-Feng Qian, Jie Yin, and Zi-Kang Zhu. Controlled morphology synthesis of β-FeOOH and the phase transition to Fe_2O_3. *Journal of Solid State Chemistry*, 178(10):3130–3136, oct 2005.

[59] A. V. Rao, R. R. Kalesh, and G. M. Pajonk. Hydrophobicity and physical properties of teos based silica aerogels using phenyltriethoxysilane as a synthesis component. *Journal of Materials Science*, 38(21):4407–4413, 2003.